Postural adaptations may contribute to the unique locomotor energetics seen in hopping kangaroos

Lauren H. Thornton[1], Taylor J.M. Dick[2], John R. Hutchinson[3], Glen A. Lichtwark[4], Craig P. McGowan[5], Jonas Rubenson[6], Alexis Wiktorowicz-Conroy[3], Christofer J. Clemente[1,2]

[1]School of Science, Technology, and Engineering, University of the Sunshine Coast, Sippy Downs, Queensland, Australia

[2]School of Biomedical Sciences, University of Queensland, St Lucia, Queensland, Australia

[3]Structure and Motion Lab, Department of Comparative Biomedical Sciences, The Royal Veterinary College, Hawkshead Lane, Hatfield, Hertfordshire, United Kingdom

[4]School of Exercise and Nutrition Science, Queensland University of Technology, Brisbane, Queensland, Australia

[5]Department of Integrative Anatomical Sciences, Keck School of Medicine University of Southern California, Los Angeles, California, USA

[6]Biomechanics Laboratory, Department of Kinesiology, The Pennsylvania State University, University Park, PA 16802, USA

Abstract

Hopping kangaroos exhibit remarkably little change in their rate of metabolic energy expenditure with locomotor speed compared to other running animals. This phenomenon may be related to greater elastic energy savings due to increasing tendon stress; however, the mechanisms which enable the rise in stress without additional muscle work remain poorly understood. In this study, we created a three-dimensional (3D) kangaroo musculoskeletal model, integrating 3D motion capture and force plate data, to analyse the kinematics and kinetics of hopping red and grey kangaroos. Using our model, we evaluated how body mass and speed influence (i) hindlimb posture, (ii) effective mechanical advantage (EMA), (iii) the associated tendon stress in the ankle extensors, and (iv) ankle work during hopping. We found that increasing ankle dorsiflexion and metatarsophalangeal plantarflexion likely played an important role in decreasing ankle EMA by altering both the muscle and external moment arms, which subsequently increased energy absorption and peak tendon stress at the ankle. Surprisingly, kangaroo hindlimb posture changes appeared to contribute to increased tendon stress, allowing more elastic energy storage at faster speeds. These posture-mediated increases in elastic energy storage and return could be a key factor enabling kangaroos to achieve energetic benefits at faster hopping speeds, but may limit the performance of large kangaroos due to the risk of tendon rupture.

Introduction

Kangaroos and other macropods are unique in both their morphology and their locomotor style. At slow speeds they use a pentapedal gait, where the forelimbs, the hindlimbs, and the tail all contact the ground, while at faster movement speeds they use their distinctive hopping gait (Dawson and Taylor 1973, O'Connor *et al.* 2014). Their uniqueness extends into their energetics of locomotion. As far back as the 19th century, researchers noticed that the metabolic cost of running in quadrupeds and bipeds, like dogs, horses and humans, increased linearly with speed (Zuntz 1897, Taylor *et al.* 1970, Heglund *et al.* 1982, Taylor *et al.* 1982). To explain why metabolic rate increased at faster running speeds among quadrupeds and bipeds, Kram and Taylor (1990) refined the 'cost of generating force' hypothesis (Taylor *et al.* 1980). They reasoned that the decrease in contact time with increased speed, reflects an increase in the rate of generating muscle force, and the rate of cross-bridge cycling (Kram and Taylor 1990). This was supported for a diverse range of running and hopping animals, suggesting that metabolic rate was inversely proportional to contact time (Kram and Taylor 1990). Yet hopping macropods appear to defy this trend. On treadmills, both red kangaroos (~20 kg) and tammar wallabies (~5 kg) showed little to no increase in the rate of oxygen consumption with increased hopping speed (Dawson and Taylor 1973, Baudinette *et al.* 1992, Kram and Dawson 1998). The underlying mechanisms explaining how macropods are able to uncouple hopping speed and energy cost is not completely understood (Thornton *et al.* 2022).

The ability to uncouple speed and energy expenditure in macropods is likely related to the behaviour of their ankle extensor muscle-tendon units, which store and return elastic strain energy (Morgan *et al.* 1978, Biewener *et al.* 2004b, McGowan *et al.* 2005). In tammar wallabies, ankle tendon stress increases with hopping speed, leading to a greater rise in elastic strain energy return than muscle work, which increases the proportion of work done by tendon recoil while muscle work remains near constant (Baudinette and Biewener 1998, Biewener *et al.* 1998). Size-related differences in ankle extensor tendon morphology (Bennett and Taylor 1995, McGowan *et al.* 2008), and the resultant low strain energy return, may explain why small (<3 kg) hopping macropods and rodents appear not to be afforded the energetic benefits observed in larger macropods (Thompson *et al.* 1980, Biewener *et al.* 1981, Biewener *et al.* 1998) (but see Christensen *et al.* (2022)). However, tendon morphology alone is insufficient to explain why large macropods can increase speed without cost, while large quadrupeds with similar tendon morphology cannot (Dawson and Webster 2010). The most obvious difference between macropods and other mammals is their hopping gait, but previously proposed mechanisms to explain how hopping could reduce the metabolic cost of generating muscle force, such as near-constant stride frequency (Heglund and Taylor 1988, Dawson

and Webster 2010) or respiratory-stride coupling (Baudinette *et al.* 1987), do not distinguish between small and large macropods, nor galloping quadrupeds (McGowan and Collins 2018).

Postural changes are another mechanism which could contribute to reduced energetic costs by altering the leverage of limb muscles. The effective mechanical advantage (EMA) is the ratio of the internal muscle-tendon moment arm (the perpendicular distance between the muscle's force-generating line-of-action and the joint centre) and the ground reaction force (GRF) moment arm (the perpendicular distance between the vector of the GRF to the joint centre). Smaller EMA requires greater muscle force to produce a given force on the ground, thereby demanding a greater volume of active muscle, and presumably greater metabolic rates, than larger EMA for the same physiology. In humans, an increase in limb flexion and decrease in limb EMA requires a greater volume of active muscle and increases the metabolic cost of running compared to walking (Biewener *et al.* 2004a, Kipp *et al.* 2018, Allen *et al.* 2022). Changes in EMA with speed are not common in quadrupedal mammals (Biewener 1989) but these are not without precedent. Elephants—one of the largest and noticeably most upright animals—do not have discrete gait transitions, but rather continuously and substantially decrease EMA in limb joints when moving faster, which has also been linked to the increase in metabolic cost of locomotion with speed (Ren *et al.* 2010, Langman *et al.* 2012). EMA is more commonly observed to change with size in terrestrial mammals. Smaller animals tend to move in crouched postures with limbs becoming progressively more extended as body mass increases (Biewener 1989). Yet, rather than metabolic cost, this postural transition appeared to be driven by the need to reduce the size-related increases in tissue stress (Dick and Clemente 2017, Clemente and Dick 2023). As a consequence of transitioning to more upright limb postures, musculoskeletal stresses in terrestrial mammals are independent of body mass (Biewener 1989, 2005).

Macropods, in contrast, maintain a crouched posture during hopping. Kram and Dawson (1998) explored whether kangaroos transitioned to a more extended limb posture with increasing speed as a potential mechanism for their constant metabolic rate, but did not detect a change in EMA at the ankle across speeds from 4.3 to 9.7 m s^{-1}. Further, ankle posture and EMA appears to vary weakly (McGowan *et al.* 2008) or not at all with body mass in macropods (Bennett and Taylor 1995, Snelling *et al.* 2017). As a consequence, stress would be expected to increase with both hopping speed and body mass. Large tendon stresses are required for rapid strain energy return (strain energy $\propto$ $stress^2$) (Biewener and Baudinette 1995). Given that tendon recoil plays a pivotal role in hopping gaits, it is perhaps unsurprising that tendon stress approaches the safe limit in larger kangaroos. The ankle extensor tendons in a moderately sized male red kangaroo (46.1 kg) operate with safety factors near two even at slow hopping speeds (3.9 m s^{-1}) (Kram and Dawson 1998), far lower than the typical safety factor of four to eight for mammalian tendons (Ker *et al.* 1988). Tendon stresses are also

unusually large in smaller kangaroos. Juvenile and adult western grey kangaroos, ranging in mass from 5.8 to 70.5 kg, all hop with gastrocnemius and plantaris tendon safety factors less than two (Snelling *et al.* 2017). Large tendon stresses may not only be a natural consequence of their crouched posture and tendon morphology, but also adaptively selected. Considering this, kangaroos may adjust their posture to increase tendon stress and its associated elastic energy return. If so, there would likely be systematic variation in kangaroo posture with speed and mass which is yet to be fully explored.

In this study, we investigated the hindlimb kinematics and kinetics in kangaroos hopping at various speeds. Specifically, we explored the relationship between changes in posture, EMA, joint work, and tendon stress across a range of hopping speeds and body masses. To do this, we built a musculoskeletal model of a kangaroo based on empirical imaging and dissection data (Fig. 1a). We used the musculoskeletal model to calculate ankle EMA throughout the stride by capturing changes in both muscle moment arm and the GRF moment arm, allowing us to explore their individual contributions. We hypothesised that (i) the hindlimb would be more crouched at faster speeds, primarily due to the distal hindlimb joints (ankle and metatarsophalangeal), independent of changes with body mass, and (ii) changes in moment arms resulting from the change in posture would contribute to the increase in tendon stress with speed, and may thereby contribute to energetic savings by increasing the amount of positive and negative work done by the ankle without requiring additional muscle work.

Results

Ground reaction forces

The stance begins with a braking phase (negative fore-aft horizontal GRF component), followed by a propulsive phase (positive fore-aft horizontal GRF component). At the transition from negative to positive, naturally the GRF was vertical, and this occurred at 42.9±26.9% of stance. The peak in vertical GRF, however, occurred at 46.4±5.3% of stance (Fig. 2a,b).

Larger kangaroos and faster speeds were associated with greater magnitudes of peak GRFs (Fig. 2a,b; Suppl. Table 2). When peak vertical GRF was normalised to body weight, peak forces ranged from 1.4 multiples of body weight (BW) to 3.7 BW per leg (mean: 2.41±0.396 BW) and increased with speed (Suppl. Fig. 2a). Smaller kangaroos may experience disproportionately greater GRFs at faster speeds (Suppl. Fig. 2b, Suppl. Table 2). The increase in GRF will tend to increase tendon stress, irrespective of changes in posture.

Kinematics and posture

Kangaroo hindlimb stance phase kinematics varied with both body mass and speed. In partial support of hypothesis (i), greater masses and faster speeds were associated with more crouched hindlimb postures (Fig. 3a,c; where crouch factor is the ratio of total limb length to pelvis to toe distance). Size-related changes in posture occurred throughout stance and were distributed as small changes among all hindlimb joints rather than a large shift in any one joint (Fig. 3d,f; Suppl. Table 3). The hip, knee and ankle tended toward more flexion, and the metatarsophalangeal (MTP) toward greater extension (plantarflexion) in larger kangaroos.

In addition to, and independent of, the change in posture with mass, there were substantial postural changes due to speed (Suppl. Table 3). Unlike with mass, speed-related changes occurred predominantly during the braking phase, and the changes were concentrated in the ankle and MTP joints, with little to no change in the proximal joints (Fig. 3c,e,g; Suppl. Table 3). There was a significant decrease in ankle plantarflexion at initial ground contact and increase in dorsiflexion at midstance at faster speeds (Fig. 3g; Suppl. Table 3). Maximum ankle dorsiflexion occurred at 44.8±4.5% of stance, and tended to occur 3.9±0.7% earlier in stance with each 1 m s^{-1} increase in speed ($P<0.001$). MTP range of motion increased with speed due to an increase in MTP plantarflexion prior to midstance rather than a change in dorsiflexion (Fig. 3g).

Effective Mechanical Advantage

Effective mechanical advantage (EMA) of the ankle decreased as the limb became more crouched. The change in EMA with mass and speed was substantial, particularly in the braking period (Fig. 2c,d). We evaluated the change in EMA at midstance, as it was approximately the point in the stride where GRF (and therefore tendon stress) was greatest. EMA at midstance decreased with body mass, although we did not detect an effect of speed (Fig. 2c,d; Suppl. Table 5), which may be due to an insignificant or undetected effect of speed on the external moment arm to the ankle, *R*. However, examining whether the decrease in EMA was caused by a decrease in the gastrocnemius and plantaris muscle moment arm, *r*, or an increase in *R*, revealed a more nuanced picture.

Speed, rather than body mass, was associated with a decrease in *r* at midstance (Suppl. Fig. 3a,b,h; Suppl. Table 5). A kangaroo travelling 1 m s^{-1} faster would decrease *r* by approximately 4.2%. The muscle moment arm reduced with speed for the full range of speeds we measured (1.99 – 4.48 m s^{-1}), with the maximum *r* occurring when the ankle was at 114.4±0.8° (Suppl. Fig. 3g). Maximum ankle dorsiflexion ranged from 114.5° in the slowest trials, to 75.8° in faster trials (Fig. 3g). The timing of the local minimum *r* at midstance coincided with the timing of peak ankle dorsiflexion.

We observed an increase in *R* with body mass, but not speed, at midstance (Suppl. Fig. 3c,d,h; Suppl. Table 5). We expected *R* to vary with both mass and speed because the increase in MTP plantarflexion prior to midstance reduced the distance between the ankle joint and the ground, which would increase *R* since the centre of pressure (CoP) at midstance remained in the same position (Suppl. Table 2). Increasing body mass by 4.6 kg or speed by 1 m s^{-1} resulted in a ~20% reduction in ankle height (vertical distance from the ground) (Suppl. Fig. 3e,f). If we consider the nonsignificant relationship between *R* (and EMA) and speed to indicate that there is no change in *R*, then it conflicts with the ankle height and CoP result. Taking both into account, we think it is more likely that there is a small, but important, change in *R*, rather than no change in *R* with speed. It may be undetectable because we expect small effect sizes compared to the measurement range and measurement error (Suppl. Fig. 3h), or be obscured by a similar change in *R* with body mass. *R* is highly dependent on the length of the metatarsal segment, which is longer in larger kangaroos (1 kg BM corresponded to ~1% longer segment, $P<0.001$, $R^2=0.449$). If *R* does indeed increase with speed, then the changes in both *R* and *r* together will tend to decrease EMA at faster speeds.

Joint moments

The change in the Achilles muscle moment arm, *r*, with speed has further implications for Achilles tendon stress, because force in the tendon is determined by the ratio of the ankle moment to *r*. As such, the decrease in *r* with speed would tend to increase tendon force (and thereby tendon stress), as would an increase in ankle moment. We found that speed, rather than mass, was associated with an increase in the maximum ankle moment (Suppl. Fig. 4; Suppl. Table 4, see supplementary material for details on other hindlimb joint moments). The range of body masses studied here may not be sufficient to detect an effect of mass on ankle moment in addition to the effect of speed.

Tendon stress

Peak Achilles tendon stress increased as minimum EMA decreased (Fig. 4a). Subtle decreases in EMA which may have been undetected in previous studies correspond to discernible increases in tendon stress. For instance, reducing EMA from 0.242 (mean minimum EMA of the slow group) to 0.206 (mean minimum EMA of the fast group) was associated with an increase in tendon stress from ~50 MPa to ~60 MPa, decreasing safety factor from 2 to 1.67 (where 1 indicates failure), which is both measurable and physiologically significant. Tendon stress increased with body mass and speed (Suppl. Table 5). Maximum stress in the ankle extensor tendons occurred at 46.8±4.9% of stance, aligning with the timing of peak vertical GRF and maximum ankle moment. Body mass did not have a significant effect on the timing of peak stress, but peak stress occurred 3.2±0.8% earlier in stance with each 1 m s^{-1} increase in speed ($P<0.001$), reflecting the timing of the peak in ankle dorsiflexion.

The increase in tendon stress with speed, facilitated in part by the change in moment arms via the shift in posture, may explain changes in ankle work (c.f. Hypothesis (ii)).

Joint work and power

An analysis of joint-level energetics showed the majority of the work per hop and power in the hindlimb was performed by the ankle joint (Fig. 5; Suppl. Table 8). The ankle performed negative work in the braking period, as kinetic and gravitational potential energy was converted to elastic potential energy by loading the ankle extensor tendons. An increase in negative ankle work was associated with the increase in tendon stress in the ankle extensors (β=0.750, SE=0.074, P<0.001, R^2=0.511). Simple linear regression indicated that the increase in negative work was associated with speed but not body mass (Fig. 6a; Suppl. Fig. 5e,f; Suppl. Table 6).

Elastic potential energy was returned to do positive work in the propulsive period as the ankle started extending prior to midstance. Positive ankle work increased with both mass and speed (Fig. 6a; Suppl. Fig. 5e,f; Suppl. Table 6), but since it increased at the same rate as negative work, critically, there was no change in net ankle work with speed (Fig. 6b; Suppl. Fig. 6e,f; Suppl. Table 6). Thus in support of hypothesis (ii), the increase in positive and negative ankle work may be due to the increase in tendon stress rather than additional muscle work.

Discussion

How does posture contribute to kangaroo energetics?

The cost of generating force hypothesis (Taylor *et al.* 1980) implies that as animals increase locomotor speed and decrease ground contact time, metabolic rate should increase (Kram and Taylor 1990). Macropods defy this trend (Dawson and Taylor 1973, Baudinette *et al.* 1992, Kram and Dawson 1998). It is likely that the use of their ankle extensor tendons set them apart from other mammals, but the underlying mechanisms are unclear (Bennett and Taylor 1995, Bennett 2000, Thornton *et al.* 2022). We hypothesised, and found, that the hindlimbs were more crouched at faster speeds, primarily due to the ankle and metatarsophalangeal joints. We propose that changes in moment arms (EMA) resulting from the change in posture would contribute to the increase in tendon stress with speed, and may thereby contribute to energetic savings by increasing the amount of positive and negative work done by the ankle, without requiring additional muscle work (Fig. 7).

Achilles tendon stress depends on extensor muscle force, which in turn depends on the muscle moment arm, ankle moment, external moment arm, and ground reaction force (GRF), assuming tendon material properties and cross-sectional area remain unchanged (Fig. 7). We detected an increase in peak ankle moment with speed independent of increases in body mass, despite the

change in the external moment arm, *R*, with mass, likely due to a dominant effect of the GRF (ankle moment = GRF · *R*). Peak GRF also naturally increased with speed together with shorter ground contact durations (Fig. 2b, Suppl. Fig. 1b). However, both the increase in ankle moment and decrease in the internal moment arm, *r,* with speed tend to increase tendon stress (stress = tendon force / cross-sectional area; tendon force = ankle moment / *r*). Although the increase in peak GRF with speed explains much of the increase in tendon stress (and strain) (Suppl. Fig. 8), the significant relationship between tendon stress and ankle EMA suggests that the increase in stress is not solely due to the greater GRFs, but that stress is also modulated by changes in posture throughout the stride (Fig. 4a). If peak GRF were constant but EMA changed from the average value of a slow hop to a fast hop, then stress would increase 18%, whereas if EMA remained constant and GRF varied by the same principles, then stress would only increase by 12%. Thus, changing posture and decreasing ground contact duration both appear to influence tendon stress for kangaroos, at least for the range of speeds we examined.

Previously, small and large macropods were reported to have consistent ankle EMA due to the muscle moment arm, *r*, and the external moment arm, *R*, scaling similarly with body mass (Fig. 4b) (Bennett and Taylor 1995). Our results, however, suggest posture may not be as consistent as previously reported; we found that EMA and moment arms varied with both mass and speed. Larger and faster kangaroos were more crouched, leading to smaller ankle EMA. We were able to explore the individual contributions to ankle EMA using our musculoskeletal model, to demonstrate that changes in the ankle and metatarsophalangeal (MTP) range of motion resulted in changes in *r* with speed, and *R* with mass, respectively. *R* (and therefore also EMA) may also increase with speed, given that the ankle joint lowers substantially closer to the ground. These effects of the moment arms were additive; combined, there was a marked decrease in ankle EMA, particularly during the early stance when the ankle extensor tendons are loaded (Fig. 2c,d).

Given that tendon stress seems to be partially controlled by EMA, kangaroos could change their posture to absorb and return greater amounts of elastic strain energy, to meet the requirements of increasing positive ankle work at faster speeds. A comparison among all the hindlimb joints suggests the ankle was primarily responsible for both the storage and release of energy during the stride (Fig. 5). Positive work increased with mass and speed, consistent with other studies in other species (Cavagna and Kaneko 1977). However, the amount of negative work absorbed during the stride also increased with speed, while, critically, net ankle work did not change, which indicates that the increase in negative work that was absorbed matched the increase in positive work that was required to move forward at more rapid speeds (Fig. 6). Indeed, we observed that all trials had a similar positive net ankle work per hop observed across all speeds (mean: 0.67 ± 0.54 J kg^{-1}). The

consistent net work observed among all speeds (combined with the consistent stride frequency) suggests that the ankle extensor muscle-tendon units were performing similar amounts of ankle work per hop independent of speed, which would predominantly be done by the tendon. As such, the change in ankle EMA appears to be a mechanism that contributes to the increase in tendon stress and positive ankle work. This mechanism may help explain why hopping macropods do not follow the energetic trends observed in other species (Dawson and Taylor 1973, Baudinette *et al.* 1992, Kram and Dawson 1998), but it does not fully resolve the cost of generating force conundrum.

Decoupling force and energy during hopping

As Achilles tendon stress increases with speed in hopping kangaroos, so too must the muscle force in the gastrocnemius and plantaris, otherwise the tendon would lengthen the muscle rather than store elastic energy. These increases in force could be achieved via increases in muscle activation, but this would also increase muscle-level energy consumption, and thus metabolic energy use. The question remains; whether there are physiologically plausible scenarios that could lead to an increase in muscle force without increasing energy use. Experimental data from hopping macropods confirm that tendon force and EMG can be decoupled, whereby greater EMG does not translate to larger forces or tendon stresses (Biewener et al. 2004b Table 2). Thus, the decoupling of energetics and speed might be explained by a muscle level change in mechanics, driven by either force-length or force-velocity relationships. Force-length effects might explain this result if muscles could operate at more favourable regions of their force-length relationship during tendon loading. The gastrocnemius and plantaris muscles of tammar wallabies do not appear to shorten considerably during hopping, but rather are suggested to act near-isometrically as a strut – however this near isometric behaviour only occurs in the second half of the stance phase (Biewener et al. 1998). This pattern in muscle fibre length does not vary with hopping speed, despite large increases in muscle tendon forces (Biewener et al. 1998).

Force-velocity effects may instead play an important role. During hopping, the gastrocnemius and plantaris activate prior to ground contact, and the majority of force development during the first half of stance is associated with muscle fibre stretch, such that the fibres undergo substantial active lengthening prior to their near-isometric behaviour (Biewener et al. 2004b Fig 3). Faster hopping speeds are also accompanied by decreased contact durations, suggesting that the rate of this muscle stretch likely increases with speed. This is supported with tendon force transducer (buckle) and kinematic data of kangaroos hopping at faster speeds (Griffiths 1989). Griffiths demonstrated that faster speeds lead to greater muscle stretch rates, the result of which enables rates of force to rise

10 times faster when compared to supramaximal isometric contractions in the same muscle. Experiments exploring single fibre energetics in frogs show that active muscle lengthening is less costly compared to isometric (Linari et al. 2003), allowing the muscle to exert tension economically. Thus, the changes in posture associated with increases in speed may allow increases in active muscle fibre stretch rates during the first half of stance, supporting increases in tendon stress, and thereby also energy storage, without increases in activation or metabolic cost. However, a detailed musculoskeletal model that incorporates individual muscle mechanical and energetic models is necessary to confirm this phenomenon.

Considerations and limitations

First, we believe it is more likely that the changes in moment arms and EMA can be attributed to speed rather than body mass, given the marked changes in joint angles and ankle height observed at faster hopping speeds. However, our sample included a relatively narrow range of body masses (13.7 to 26.6 kg) compared to the potential range (up to 80 kg), limiting our ability to entirely isolate the effects of speed from those of mass. Future research should examine a broader range of body sizes. Second, kangaroos studied here only hopped at relatively slow speeds, which bounds our estimates of EMA and tendon stress to a less critical region. As such, we were unable to assess tendon stress at fast speeds, where increased forces would reduce tendon safety factors closer to failure. A different experimental or modelling approach may be needed, as kangaroos in enclosures seem unwilling to hop faster over force plates. Finally, we did not determine whether the EMA of proximal hindlimb joints (which are more difficult to track via surface motion capture markers) remained constant with speed. Although the hip and knee contribute substantially less work than the ankle joint (Fig. 5), the majority of kangaroo skeletal muscle is located around these proximal joints. A change in EMA at the hip or knee could influence a larger muscle mass than at the ankle, potentially counteracting or enhancing energy savings in the ankle extensor muscle-tendon units. Further research is needed to understand how posture and muscles throughout the whole body contribute to kangaroo energetics.

Why are macropods unique?

No other mammals are known to achieve the same energetic feat as macropods, despite similar tendons or stride parameters (Thornton *et al.* 2022), but macropods are unique in other ways. Kangaroos operate at much lower ankle EMA values than other large mammalian species (Fig. 4b).

Mammals >18 kg tend to operate with EMA values 0.5 to 1.2. The only mammals with comparable EMA values to kangaroos are rodents <1 kg (Fig. 4b) (Biewener 1990), such as kangaroo rats which have relatively thicker tendons that may be less suited for recovering elastic strain energy (Biewener and Blickhan 1988) (but see: Christensen *et al.* (2022)). Fig. 4a shows the non-linear relationship between tendon stress and EMA in kangaroos, quadrupeds and humans. The range of EMA estimates for other mammals suggest they operate in the region of this curve where large changes in EMA would only produce small changes in stress. This implies EMA modulation in other species is not as effective a mechanism to increase tendon stress with increased running speed as that observed in kangaroos.

Were macropods performance- or size-limited?

The morphology and hopping gait that make kangaroos supremely adapted for economical locomotion likely also have several performance limitations. One possible consequence is a predicted reduction in manoeuvrability (Biewener 2005). The high compliance of the Achilles tendon would limit the ability to rapidly accelerate, owing to the time lag between muscle force production and the transmission of this force to the environment. A second important limitation is the requirement for kangaroos to operate at large tendon stresses. Previous research has suggested that kangaroos locomote at dangerously low safety factors for tendon stress, predicted to be between 1-2 for large kangaroos (Kram and Dawson 1998, McGowan *et al.* 2008, Snelling *et al.* 2017, Thornton *et al.* 2022). Our new insights into the mass and speed modulated changes in EMA suggest that these safety factors may be even lower, likely limiting the maximum body mass that hopping kangaroos can achieve. This suggests that previous projections of tendon stress may have overestimated the body mass at which tendons reach their safety limit ('safety factor' of 1). Snelling *et al.* (2017) and McGowan *et al.* (2008) estimated the maximum body mass to remain above this limit was approximately 150 kg, but even if we consider this is a conservative prediction, it is far lower than the estimated mass of extinct macropodids (up to 240 kg (Helgen *et al.* 2006, Janis *et al.* 2023). Thus we expect there must be a body mass where postural and gait changes shift from contributing to stress to mitigating it (Dick and Clemente 2017).

This study highlights how EMA may be more adjustable than previously assumed, and how musculoskeletal modelling and simulation approaches can provide insights into direct links between form and function which are often challenging to determine from experiments alone.

Methods

Animals and data collection

Hopping data for red and eastern grey kangaroos was collected at Brisbane's Alma Park Zoo in Queensland, Australia, in accordance with approval by the Ethics and Welfare Committee of the Royal Veterinary College; approval number URN 2010 1051. The dataset includes 16 male and female kangaroos ranging in body mass from 13.7 to 26.6 kg (20.9 ± 3.4 kg). Two juvenile red (*Macropus rufus*) and 11 grey kangaroos (*Macropus giganteus*) were identified, while the remaining three could not be differentiated as either species. Body mass was determined in several ways, primarily by measurements of the kangaroos standing stationary on the force plate. If the individual did not stop on the force plate, and forward velocity was constant, then body mass was determined by dividing the total vertical impulse (force integrated across time) across a constant velocity hop cycle (foot strike to foot strike) by the total hop cycle time and further dividing by gravitational acceleration. Finally, if neither of these approaches were sufficient, we interpolated from the relationship between leg marker distances (as proxy for segment lengths) and body mass. These methods produce estimates of body masses close to stationary measurements, where both were available.

Experimental protocol

Kangaroos hopped down a runway (~10x1.5 m) that was constructed in their enclosure using hessian cloths and stakes (Suppl. Video 1). The kangaroos elected to hop between 1.99 and 4.48 m s^{-1}, with a range of speeds and number of trials for each individual (Suppl. Fig. 9). The runway was open at both ends with two force plates (Kistler custom plate (60x60 cm) and AMTI Accugait plate (50x50 cm)) set sequentially in the centre and buried flush with the surface. The force plates recorded ground reaction forces (GRF) in the vertical, horizontal and lateral directions.

A 6-camera 3D motion capture system (Vicon T160 cameras), recorded by Nexus software (Vicon, Oxford, UK) at 200 Hz, was used to record kinematic data. Reflective markers were placed on the animals over the estimated hip, knee, ankle, metatarsophalangeal (MTP) joints; the distal end of phalanx IV; the anterior tip of the ilium; and the base of the tail (Fig. 1a). Force plate data was synchronously recorded at 1000 Hz via an analogue to digital board integrated with the Vicon system.

Data analysis

We calculated the stride length from the distance between the ankle or MTP marker coordinates at equivalent time points in the stride. The stance phase was defined as the period when the vertical

GRF was greater than 2% of the peak GRF. We determined ground contact duration and total stride duration from the frame rate (200 Hz) and the number of frames from contact to take-off (contact duration) and contact to contact (stride duration), respectively, and calculated the stride frequency. Stride parameter results are detailed in the supplementary material.

In most trials, the stride before and after striking the force plate was visible, providing a total of 173 strides. If two strides were present in a trial, we took the average of the two strides for that trial. Trials were excluded if only one foot landed on the force plate or if the feet did not land near-simultaneously, to give a total of 100 trials, with variety in the number of trials per kangaroo (Suppl Fig. 9). We did not include trials where the kangaroo started from or stopped on the force plate. We assumed GRF was equally shared between each leg and divided the vertical, horizontal and lateral forces in half, and calculated all results for one leg. We normalised GRF by body weight.

The fore-aft movement of the centre of pressure (CoP) was recorded by the force plate within the motion capture coordinate system (Fig. 1b). We assumed that the force was applied along phalanx IV and that there was no medial-lateral movement of the CoP. It was necessary to assume the CoP was fixed along the medial-lateral axis because when two feet landed on the force plate, the lateral forces on each foot were not recorded, and indeed should have cancelled if the forces were symmetrical (i.e. if the kangaroo was hopping in a straight path and one foot is not in front of the other). We only used symmetrical trials to ensure reliable measures of the anterior-posterior movement of the CoP.

We calculated the hopping velocity and acceleration of the kangaroo in each trial from the position of the pelvis marker, as this marker was close to the centre of mass and there should have been minimal skin movement artefact. Position data were smoothed using the 'smooth.spline' function in R (version 3.6.3). The average locomotor speed of the trial was taken as the mean horizontal component of the velocity during the aerial phase before and after the stance phase.

Building a kangaroo musculoskeletal model

We created a musculoskeletal model based on the morphology of a kangaroo for use in OpenSim (v3.3; Seth *et al.* (2018)) (Fig. 1a). The skeletal geometry was determined from a computed tomography (CT) scan of a mature western grey kangaroo (MorphoSource.org, Duke University, NC, USA). Western grey kangaroos are morphologically similar to eastern grey and red kangaroos (Thornton *et al.* 2022).

We extracted the skeletal components from the CT scan using Dragonfly (Version 2020.2, Object Research Systems (ORS) Inc., Montreal, Canada) and partitioned the hindlimb into five segments

(pelvis, femur, tibia, metatarsals and calcaneus, and phalanges). The segments were imported into Blender (version 3.0.0, https://www.blender.org/; Amsterdam, Netherlands) to clean and smooth the bones, align the vertebrae, and export the segments as meshes. We imported the meshes into Rhinoceros (version 6.0, Robert McNeel & Associates, Seattle, WA, USA) to construct the framework of the movement system.

All joints between segments were modelled as hinge joints which constrain motion to a single plane and one degree of freedom (DOF), except the hips which were modelled as ball-and-socket joints with three DOF. The joints were restricted to rotational (no translational) movement. The joints were marked with an origin (joint centre) and coordinate system determined by the movement of the segment (x is abduction/adduction, y is pronation/supination, z is extension/flexion). The limb bones and joints from one leg were mirrored about the sagittal plane to ensure bilateral symmetry.

The segment masses for a base model were determined from measurements of eastern grey and red kangaroos provided in Hopwood (1976). Cylinders set to the length and mass of each segment were used to approximate the segment centre of mass and moments of inertia.

We scaled the model to the size, shape and mass of each kangaroo using the OpenSim scale tool and kangaroo markers. A static posture was defined based on the 3D positions of the markers at midstance. Each segment was scaled separately, allowing for different scaling factors across segments but preserving mass distribution. The markers with less movement of the skin over the joint (e.g. the MTP marker) were more highly weighted than the markers with substantial skin movement (e.g. the hip and knee markers) in the scaling tool.

Joint kinematics and mechanics

We used inverse kinematics to determine time-varying joint angles during hopping. Inverse kinematics is an optimisation routine which simulates movement by aligning the model markers with the markers in the kinematic data for each time step (Suppl. Video 2). We adjusted the weighting on the markers based on the confidence and consistency in the marker position relative to the skeleton. The model movement from inverse kinematics was combined with GRFs in an inverse dynamics analysis in OpenSim to calculate net joint moments for the hip, knee, ankle and MTP joints throughout stance phase. Joint moments were normalised to body weight and leg length (Fig. 1a).

We calculated instantaneous joint powers (joint work) for each of the hindlimb joints over the stance phase of hopping as the product of joint moment (not normalised) and joint angular velocity. To determine joint work, we integrated joint powers with respect to time over discrete periods of positive and negative work, consistent with Dick *et al.* (2019). For the stance duration of each hop,

all periods of positive work were summed and all periods of negative work were summed to determine the positive work, negative work, and net work done at each of the hindlimb joints for a hop cycle. Joint work was normalised to body mass.

Posture and EMA

We evaluated overall hindlimb posture to determine how crouched or upright the hindlimbs were during the stance phase of hopping. The total hindlimb length was determined as the sum of all segment lengths between the joint centres, from the toe to ilium (Fig. 1a). The crouch factor (CF) was calculated as the distance between the toe and the ilium marker divided by the total hindlimb length. Larger CF values indicated extended limbs whereas smaller CF values indicated more crouched postures.

We calculated the effective mechanical advantage (EMA) at the ankle as the muscle moment arm of the combined gastrocnemius and plantaris tendon, *r*, divided by the external moment arm, *R* (perpendicular distance between the GRF vector and the ankle joint) (Fig. 1b). We dissected (with approval from University of the Sunshine Coast Ethics Committee, ANE2284) a road-killed 27.6 kg male eastern grey kangaroo and used this, combined with published anatomy on the origin and insertion sites, to determine the ankle extensor muscle-tendon unit paths on the skeleton in OpenSim (Bauschulte 1972, Hopwood and Butterfield 1976, Hopwood and Butterfield 1990). The value *r* to the gastrocnemius and plantaris tendons for all possible ankle angles were determined from OpenSim and scaled to the size of each kangaroo, while *R* was calculated as the perpendicular distance between the ankle marker and the GRF vector at the CoP.

Tendon stress

Ankle extensor tendon forces were estimated as the time-varying ankle moment divided by the time varying Achilles tendon moment arm. Achilles tendon cross-sectional area was determined as the sum of the gastrocnemius and plantaris tendon cross-sectional areas, which were determined for each kangaroo body mass based on area-mass regressions from Snelling *et al.* (2017). Forces were divided by tendon cross-sectional area to calculate tendon stress. We excluded the third ankle extensor tendon (flexor digitorum longus), which has a shorter muscle moment arm and which stores ~10% of strain energy of the ankle extensors in tammar wallabies as it is primarily involved in foot placement rather than energy storage (Biewener and Baudinette 1995).

Statistics

We used multiple linear regression (lm function in R, v. 3.6.3, Vienna, Austria) to determine the effects of body mass and speed on the stride parameters, ground reaction forces, joint angles and CF, joint moments, joint work and power, and tendon stress. We considered the interaction of body

mass and speed first, and removed the interaction term from the linear model if the interaction was not significant. Effects were considered significant at the $p<0.05$ level. Each trial was treated individually, and species was not used as a factor in the analysis as there was no systematic difference in outcome measures between kangaroo species. The data was grouped into body mass (small 17.6±2.96 kg, medium 21.5±0.74 kg, large 24.0±1.46 kg) and speed (slow 2.52±0.25 m s^{-1}, medium 3.11±0.16 m s^{-1}, fast 3.79±0.27 m s^{-1}) subsets for display purposes only.

Acknowledgements

We thank the Brisbane Alma Park Zoo for hosting and facilitating this work; particularly Dena Loveday and Heather Hesterman. Matthew Brown provided access to the CT scan, the collection of which was funded by the Texas Vertebrate Paleontology Collections. Megan Johnston and Rachel Lyons from Wildcare Australia provided road-killed kangaroos for muscle dissection. We also thank Alex Muir from Logemas for loan of the 3D motion capture system. We also thank the reviewers for their suggestions and edits to the manuscript, their contribution greatly strengthened this manuscript.

Funding

This work was supported by: Australian Government Research Training Program Scholarship and ISB Comparative Neuromuscular Biomechanics Technical Group Student Grant-in-Aid of Research to LHT; Biotechnology and Biological Sciences Research Council Grant (BB/F000863) to JRH; Journal of Experimental Biology Travelling Fellowship to CPM; Australian Research Council Discovery Project Grant to CJC, TD and CM (DP230101886).

References

Allen, S. P., O. N. Beck, and A. M. Grabowski. 2022. Evaluating the 'cost of generating force' hypothesis across frequency in human running and hopping. Journal of Experimental Biology **225**:jeb244755.

Baudinette, R. V., and A. A. Biewener. 1998. Young wallabies get a free ride. Nature **395**:653-654.

Baudinette, R. V., B. J. Gannon, W. B. Runciman, S. Wells, and J. B. Love. 1987. Do cardiorespiratory frequencies show entrainment with hopping in the tammar wallaby? Journal of Experimental Biology **129**:251-263.

Baudinette, R. V., G. K. Snyder, and P. B. Frappell. 1992. Energetic cost of locomotion in the tammar wallaby. American Journal of Physiology **262**:771-778.

Bauschulte, C. 1972. Morphologische und biomechanische Grundlagen einer funktionellen Analyse der Muskeln der Hinterextremität (Untersuchung an quadrupeden Affen und Känguruhs). Zeitschrift für Anatomie und Entwicklungsgeschichte **138**:167–214.

Bennett, M. B. 2000. Unifying principles in terrestrial locomotion: do hopping Australian marsupials fit in? Physiological and Biochemical Zoology **73**:726-735.

Bennett, M. B., and G. C. Taylor. 1995. Scaling of elastic strain energy in kangaroos and the benefits of being big. Nature **378**:56-59.

Biewener, A. A. 1989. Scaling body support in mammals: limb posture and muscle mechanics. Science **245**:45-48.

Biewener, A. A. 1990. Biomechanics of mammalian terrestrial locomotion. Science **250**:1097-1103.

Biewener, A. A. 2005. Biomechanical consequences of scaling. Journal of Experimental Biology **208**:1665-1676.

Biewener, A. A., R. M. Alexander, and N. C. Heglund. 1981. Elastic energy storage in the hopping of kangaroo rats (*Dipodomys spectabilis*). Journal of Zoology **195**:369-383.

Biewener, A. A., and R. Baudinette. 1995. *In vivo* muscle force and elastic energy storage during steady-speed hopping of tammar wallabies (*Macropus eugenii*). Journal of Experimental Biology **198**:1829-1841.

Biewener, A. A., and R. Blickhan. 1988. Kangaroo rat locomotion: design for elastic energy storage or acceleration? Journal of Experimental Biology **140**:243-255.

Biewener, A. A., C. T. Farley, T. J. Roberts, and M. Temaner. 2004a. Muscle mechanical advantage of human walking and running: implications for energy cost. Journal of Applied Physiology **97**:2266-2274.

Biewener, A. A., D. D. Konieczynski, and R. V. Baudinette. 1998. *In vivo* muscle force-length behavior during steady-speed hopping in tammar wallabies. Journal of Experimental Biology **201**:1681-1694.

Biewener, A. A., C. McGowan, G. M. Card, and R. V. Baudinette. 2004b. Dynamics of leg muscle function in tammar wallabies (*M. eugenii*) during level versus incline hopping. Journal of Experimental Biology **207**:211-223.

Cavagna, G. A., and M. Kaneko. 1977. Mechanical work and efficiency in level walking and running. The Journal of Physiology **268**:467-481.

Christensen, B. A., D. C. Lin, M. J. Schwaner, and C. P. McGowan. 2022. Elastic energy storage across speeds during steady-state hopping of desert kangaroo rats (Dipodomys deserti). Journal of Experimental Biology **225**.

Clemente, C. J., and T. J. M. Dick. 2023. How scaling approaches can reveal fundamental principles in physiology and biomechanics. Journal of Experimental Biology **226**.

Dawson, T. J., and C. R. Taylor. 1973. Energetic cost of locomotion in kangaroos. Nature **246**:313-314.

Dawson, T. J., and K. N. Webster. 2010. Energetic characteristics of macropodoid locomotion. Pages 99-108 *in* G. Coulson and M. Eldridge, editors. Macropods: the biology of kangaroos, wallabies and rat-kangaroos. CSIRO Publishing, Collingwood Vic. Australia.

Dick, T. J. M., and C. J. Clemente. 2017. Where have all the giants gone? How animals deal with the problem of size. PLoS Biology **15**:e2000473.

Dick, T. J. M., L. K. Punith, and G. S. Sawicki. 2019. Humans falling in holes: adaptations in lower-limb joint mechanics in response to a rapid change in substrate height during human hopping. Journal of the Royal Society Interface **16**:20190292.

Griffiths, R. 1989. The mechanics of the medial gastrocnemius muscle in the freely hopping wallaby (*Thylogale billardierii*). Journal of Experimental Biology **147**:439-456.

Heglund, N. C., G. A. Cavagna, and C. R. Taylor. 1982. Energetics and mechanics of terrestrial locomotion. III. Energy changes of the centre of mass as a function of speed and body size in birds and mammals. Journal of Experimental Biology **97**:41-56.

Heglund, N. C., and C. R. Taylor. 1988. Speed, stride frequency and energy cost per stride: how do they change with body size and gait? Journal of Experimental Biology **138**:301-318.

Helgen, K. M., R. T. Wells, B. P. Kear, W. R. Gerdtz, and T. F. Flannery. 2006. Ecological and evolutionary significance of sizes of giant extinct kangaroos. Australian Journal of Zoology **54**:293-303.

Hopwood, P. R. 1976. The quantitative anatomy of the kangaroo. University of Sydney.

581 Hopwood, P. R., and R. M. Butterfield. 1976. The musculature of the proximal pelvic limb of the
582 eastern grey kangaroo *Macropus major* (Shaw) *Macropus giganteus* (Zimm). Journal of
583 Anatomy **121**:259-277.
584 Hopwood, P. R., and R. M. Butterfield. 1990. The locomotor apparatus of the crus and pes of the
585 eastern gray kangaroo, *Macropus giganteus*. Australian Journal of Zoology **38**:397-413.
586 Janis, C. M., A. M. O'Driscoll, and B. P. Kear. 2023. Myth of the QANTAS leap: perspectives on the
587 evolution of kangaroo locomotion. Alcheringa: An Australasian Journal of Palaeontology
588 **47**:1-15.
589 Ker, R. F., R. M. Alexander, and M. B. Bennett. 1988. Why are mammalian tendons so thick? Journal
590 of Zoology **216**:309-324.
591 Kipp, S., A. M. Grabowski, and R. Kram. 2018. What determines the metabolic cost of human running
592 across a wide range of velocities? Journal of Experimental Biology **221**.
593 Kram, R., and T. J. Dawson. 1998. Energetics and biomechanics of locomotion by red kangaroos
594 (*Macropus rufus*). Comparative Biochemistry and Physiology, Part B **120**:41-49.
595 Kram, R., and C. R. Taylor. 1990. Energetics of running: a new perspective. Nature **346**:265-267.
596 Langman, V. A., M. F. Rowe, T. J. Roberts, N. V. Langman, and C. R. Taylor. 2012. Minimum cost of
597 transport in Asian elephants: Do we really need a bigger elephant? Journal of Experimental
598 Biology **215**:1509-1514.
599 Linari, M., R. Woledge, and N. Curtin. 2003. Energy storage during stretch of active single fibres from
600 frog skeletal muscle. The Journal of Physiology **548**:461-474.
601 McGowan, C. P., R. V. Baudinette, and A. A. Biewener. 2005. Joint work and power associated with
602 acceleration and deceleration in tammar wallabies (*Macropus eugenii*). Journal of
603 Experimental Biology **208**:41-53.
604 McGowan, C. P., and C. E. Collins. 2018. Why do mammals hop? Understanding the ecology,
605 biomechanics and evolution of bipedal hopping. Journal of Experimental Biology
606 **221**:jeb161661.
607 McGowan, C. P., J. Skinner, and A. A. Biewener. 2008. Hind limb scaling of kangaroos and wallabies
608 (superfamily Macropodoidea): implications for hopping performance, safety factor and
609 elastic savings. Journal of Anatomy **212**:153-163.
610 Morgan, D. L., U. Proske, and D. Warren. 1978. Measurements of muscle stiffness and the
611 mechanism of elastic storage of energy in hopping kangaroos. The Journal of Physiology
612 **282**:253-261.
613 O'Connor, S. M., T. J. Dawson, R. Kram, and J. M. Donelan. 2014. The kangaroo's tail propels and
614 powers pentapedal locomotion. Biology Letters **10**:20140381.
615 Ren, L., C. E. Miller, R. Lair, and J. R. Hutchinson. 2010. Integration of biomechanical compliance,
616 leverage, and power in elephant limbs. Proceedings of the National Academy of Sciences -
617 PNAS **107**:7078-7082.
618 Seth, A., J. L. Hicks, T. K. Uchida, A. Habib, C. L. Dembia, J. J. Dunne, C. F. Ong, M. S. DeMers, A.
619 Rajagopal, M. Millard, S. R. Hamner, E. M. Arnold, J. R. Yong, S. K. Lakshmikanth, M. A.
620 Sherman, J. P. Ku, and S. L. Delp. 2018. OpenSim: simulating musculoskeletal dynamics and
621 neuromuscular control to study human and animal movement. PLoS Computational Biology
622 **14**:e1006223.
623 Snelling, E. P., A. A. Biewener, Q. Hu, D. A. Taggart, A. Fuller, D. Mitchell, S. K. Maloney, and R. S.
624 Seymour. 2017. Scaling of the ankle extensor muscle-tendon units and the biomechanical
625 implications for bipedal hopping locomotion in the post-pouch kangaroo *Macropus*
626 *fuliginosus*. Journal of Anatomy **231**:921-930.
627 Taylor, C. R., N. C. Heglund, and G. M. Maloiy. 1982. Energetics and mechanics of terrestrial
628 locomotion. I. Metabolic energy consumption as a function of speed and body size in birds
629 and mammals. Journal of Experimental Biology **97**:1-21.

Taylor, C. R., N. C. Heglund, T. A. McMahon, and T. R. Looney. 1980. Energetic cost of generating muscular force during running: a comparison of large and small animals. Journal of Experimental Biology **86**:9-18.

Taylor, C. R., K. Schmidt-Nielsen, and J. L. Raab. 1970. Scaling of energetic cost of running to body size in mammals. American Journal of Physiology **219**:1104-1107.

Thompson, S. D., R. E. MacMillen, E. M. Burke, and C. R. Taylor. 1980. The energetic cost of bipedal hopping in small mammals. Nature **287**:223-224.

Thornton, L. H., T. J. M. Dick, M. B. Bennett, and C. J. Clemente. 2022. Understanding Australia's unique hopping species: a comparative review of the musculoskeletal system and locomotor biomechanics in Macropodoidea. Australian Journal of Zoology **69**:136-157.

Zuntz, N. 1897. Ueber den Stoffverbrauch des Hundes bei Muskelarbeit. Arch. Ges. Physiol. **68**:191-211.

Figures

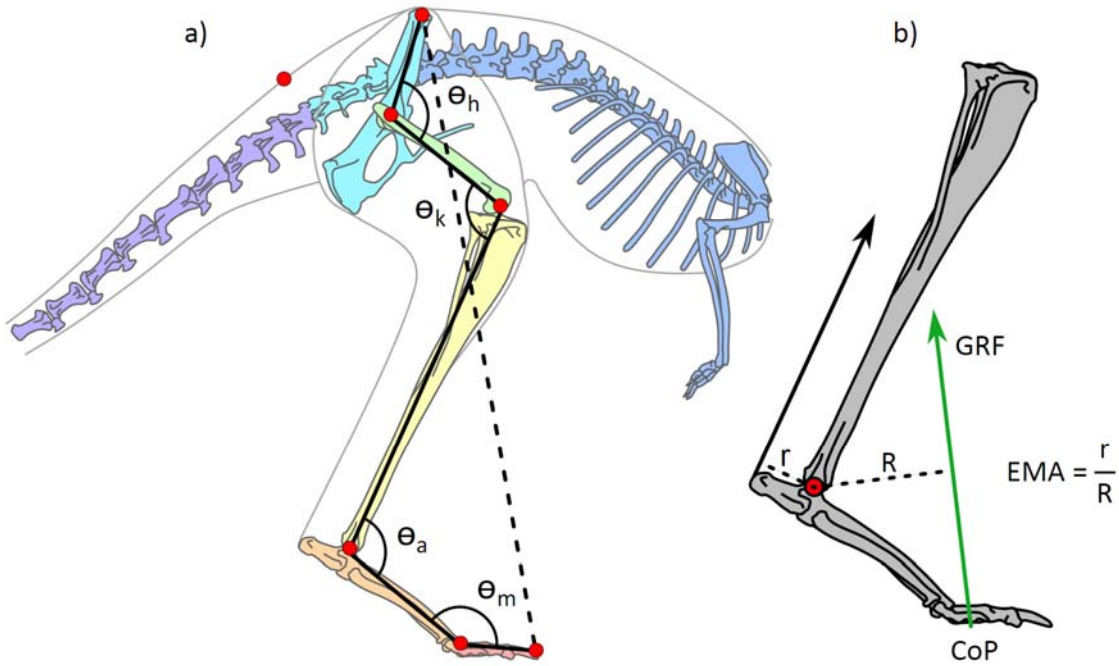

Figure 1: (a) Illustration of the kangaroo model. Total leg length was calculated as the sum of the segment lengths (solid black lines) in the hindlimb and compared to the pelvis-to-toe distance (dashed line) to calculate the crouch factor. Joint angles were determined for the hip, h, knee, k, ankle, a, and metatarsophalangeal, m, joints. The model markers (red circles) indicate the position of the reflective markers placed on the kangaroos in the experimental trials and were used to characterise the movement of segments in the musculoskeletal model. (b) Illustration of ankle effective mechanical advantage, EMA, muscle moment arm, r, and external moment arm, R, as the perpendicular distance to the Achilles tendon line of action and ground reaction force (GRF) vector, respectively. The centre of pressure (CoP) was tracked in the fore-aft direction.

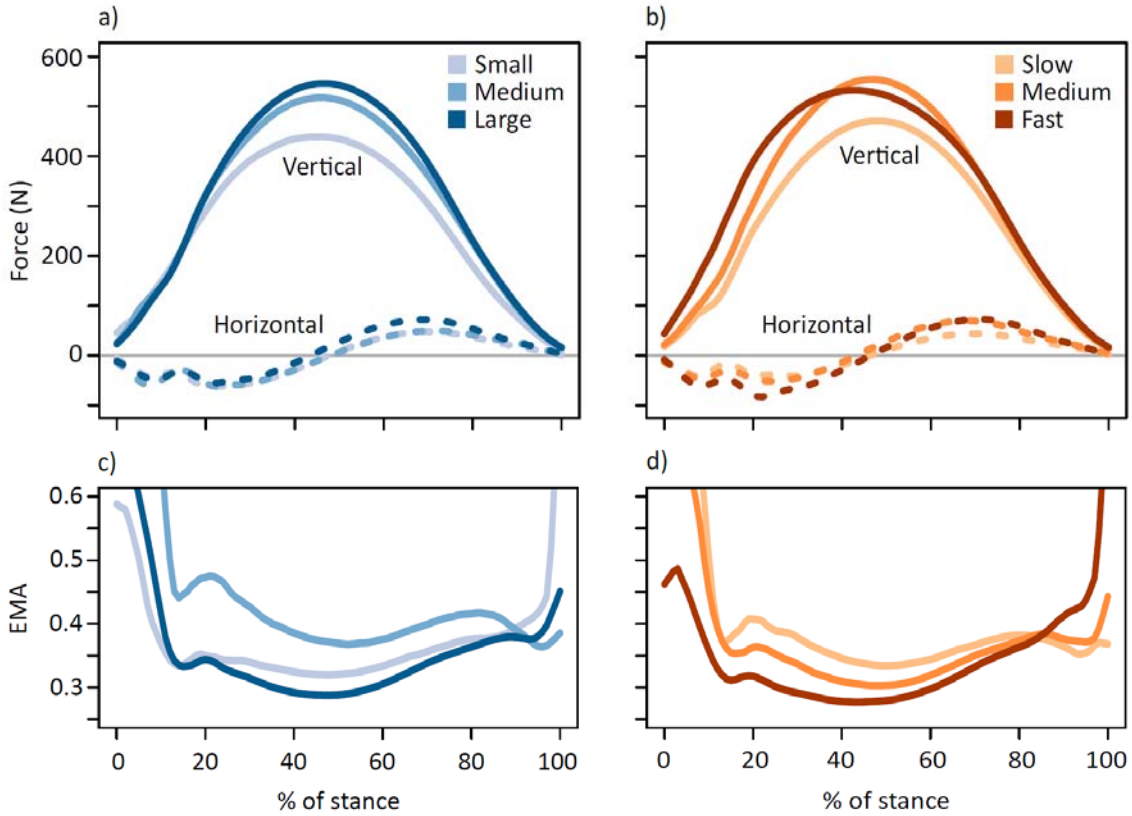

Figure 2: Horizontal fore-aft (dashed lines) and vertical (solid lines) components of the ground reaction force (GRF) (a) coloured by body mass subsets (small 17.6±2.96 kg, medium 21.5±0.74 kg, large 24.0±1.46 kg) and (b) coloured by speed subsets (slow 2.52±0.25 m s^{-1}, medium 3.11±0.16 m s^{-1}, fast 3.79±0.27 m s^{-1}). In (a) and (b) the medial-lateral component of the GRF is not shown as it remained close to zero, as expected for animals moving in a straight-line path. Lower panels show average time-varying EMA for the ankle joint subset by (c) body mass and (d) speed.

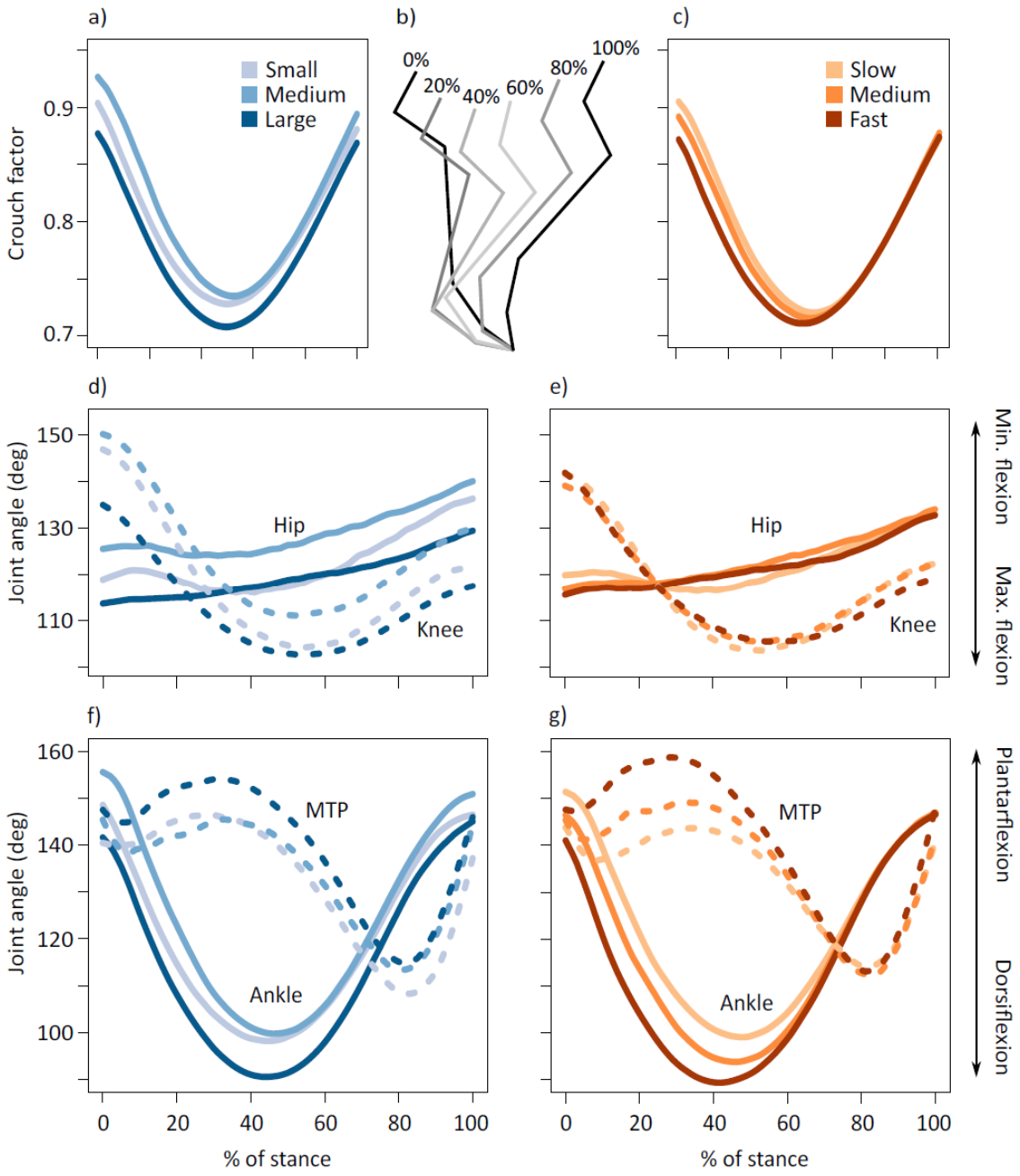

Figure 3: Average time-varying crouch factor (see Fig. 1a) of the kangaroo hindlimb grouped by (a) body mass and (c) speed. Position of the limb segments during % stance intervals (b). Average time-varying joint angles for the hip (solid lines) and knee (dashed lines) displayed for kangaroos grouped by (d) body mass and (e) speed. Average time-varying joint angles for the ankle (solid lines) and metatarsophalangeal (MTP) joints (dashed lines) displayed for kangaroos grouped by (f) body mass and (g) speed. For (f-g), increased plantarflexion represents a decrease in joint flexion, while increased dorsiflexion represents increased flexion of the joint. Body mass subsets: small 17.6±2.96 kg, medium 21.5±0.74 kg, large 24.0±1.46 kg. Speed subsets: slow 2.52±0.25 m s^{-1}, medium 3.11±0.16 m s^{-1}, fast 3.79±0.27 m s^{-1}.

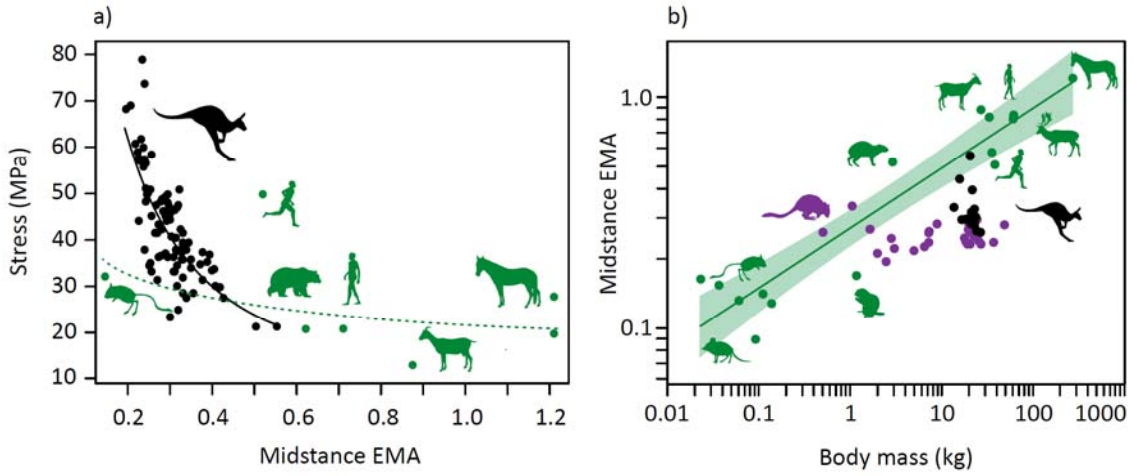

Figure 4: (a) Relationship between ankle effective mechanical advantage, EMA, at midstance and Achilles tendon stress (stress = 11.6 $EMA^{-1.04}$, R^2=0.593) (black), with other mammals (green). (b) Scaling of mean ankle EMA at midstance for each individual kangaroo against body mass (black), with data for a wider range of macropods (purple) (Bennett and Taylor 1995), and other mammals (green, EMA = 0.269 $M^{0.259}$, shaded area 95% confidence interval) (Biewener 1990) shown.

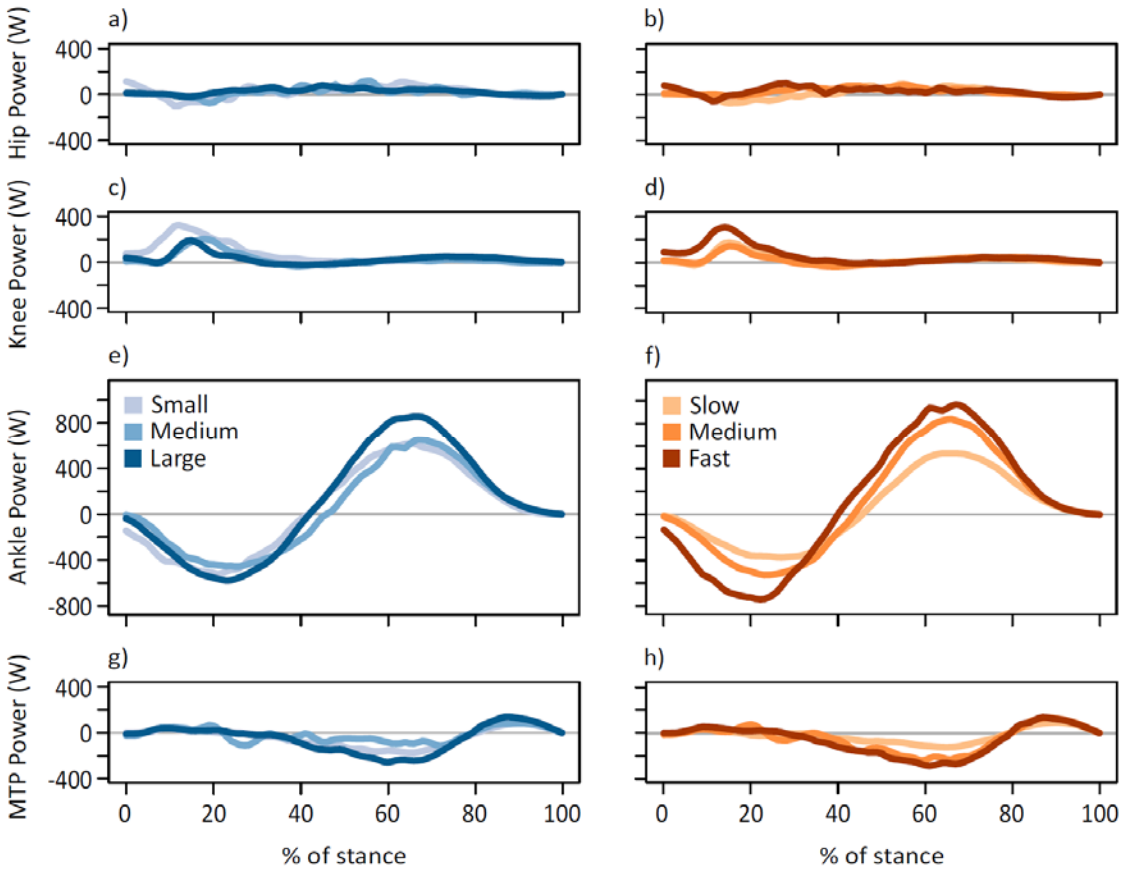

Figure 5: Average time-varying joint powers for the hip (a,b), knee (c, d), ankle (e, f), and MTP (g, h) displayed for kangaroos grouped by body mass (a, c, e, g) and speed (b, d, f, h). Power in all panels is set to the same scale. Body mass subsets: small 17.6±2.96 kg, medium 21.5±0.74 kg, large 24.0±1.46 kg. Speed subsets: slow 2.52±0.25 m s^{-1}, medium 3.11±0.16 m s^{-1}, fast 3.79±0.27 m s^{-1}.

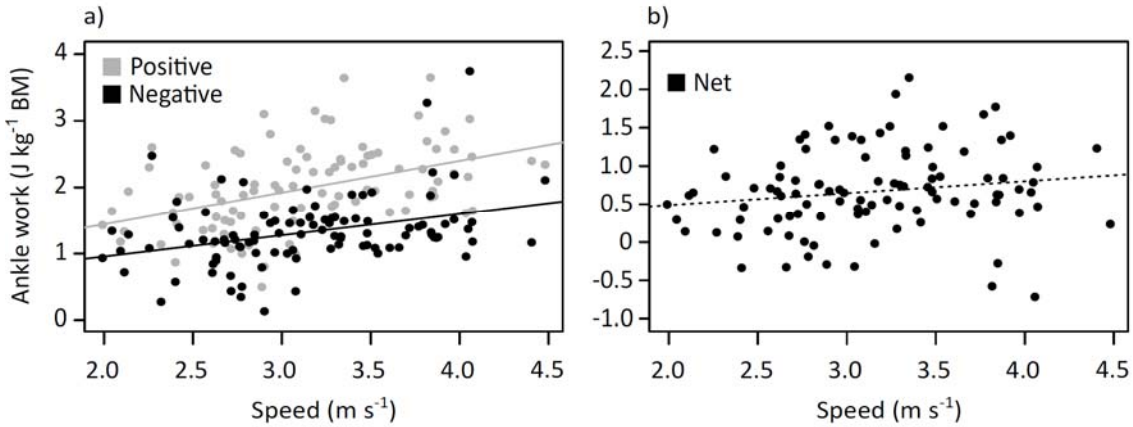

Figure 6: Variation with speed of (a) positive and negative ankle work, and (b) net ankle work per hop.

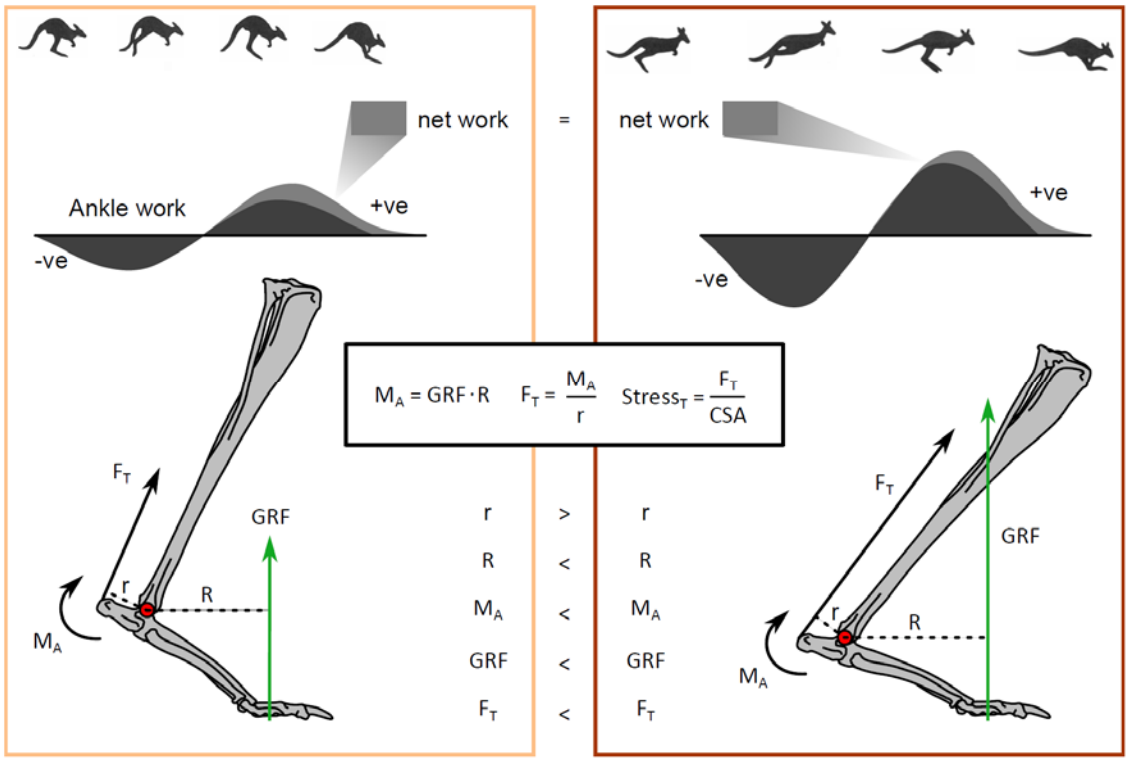

Figure 7: How the relationship between posture and speed is proposed to change tendon stress. Forces are not to scale and joint angles are exaggerated for illustrative clarity. A slow hop (left panel) compared to a fast hop (right panel). The increase in ground reaction force (GRF) with speed, while a more crouched posture changes the muscle moment arm, r, and external moment arm, R, which allows the ankle to do more negative work (storing elastic potential energy in the tendons due to greater tendon stresses), without increasing net work, and thereby metabolic cost. Ankle moment was calculated by OpenSim and includes inertial terms.

Supplementary Results

Stride parameters

Hopping speed ranged from 1.99 to 4.48 m s^{-1}. Larger kangaroos tended to hop at slightly faster speeds (B=0.048, SE=0.018, P=0.009, R^2=0.057), and due to this weak relationship between body mass and speed, both variables were considered in multiple linear regression models to determine their relative effects on the outcome measures (see Table 1).

Faster speeds were associated with a greater magnitude of acceleration in the braking period of the stance phase, i.e. minimum horizontal acceleration and maximum vertical acceleration (Suppl. Fig. 1a). There was no significant relationship between body mass and acceleration; however, there was a significant interaction between body mass and speed on maximum vertical acceleration, whereby smaller kangaroos had a greater change in vertical acceleration between slower and faster hopping speeds than larger kangaroos (Table 1).

Body mass and speed had different effects on ground contact duration (Table 1). There was a slightly greater (or longer) contact duration in larger kangaroos. A stronger, opposing relationship was found with speed, and as speed increased, contact duration decreased. The relatively tight correlation between contact duration and hopping speed (R^2=0.73) could prove useful for predicting speed when contact duration can be accurately measured. In Suppl. Fig. 1b we combined our data with red kangaroo data from Kram and Dawson (1998) to extend the predictive range of both studies.

Larger kangaroos hopped with longer strides and lower frequencies than smaller kangaroos (Table 1), and stride length also increased with speed (Suppl. Fig. 1c). We found a significant decrease in stride frequency with mass and an increase with speed, if we did not consider the interaction term (Suppl. Fig. 1d). However, a significant interaction between body mass and speed suggests that larger kangaroos relied more on increases in stride frequency to increase hopping speed compared to smaller kangaroos (Table 1).

Ground reaction forces

It is commonly assumed that the GRF is vertical and at a maximum at midstance or 50% of stance (Bennett and Taylor 1995, Kram and Dawson 1998, McGowan *et al.* 2008, Snelling *et al.* 2017) but our results suggest it occurred earlier, at 42.9±26.9% of stance, and the wide range suggests such assumptions should be used with caution.

Kinematics and posture

Kangaroos were maximally crouched at midstance, with crouch factor (CF) reaching a minimum at 50.1±4.2% of stance. Crouch factor (CF) at initial ground contact decreased at faster speeds,

although the limb was similarly flexed during midstance (P=0.295). Consequently, CF changed less at faster speeds than slower speeds.

Larger kangaroos had smaller hip and knee ranges of motion (ROM) compared to smaller kangaroos (Fig. 3d; Suppl. Table 3). In the distal hindlimb, ankle ROM increased with body mass, largely owing to an increase in dorsiflexion at midstance (Fig. 3f; Suppl. Table 3). The ROM of the MTP joint did not change with body mass; however, there was both an increase in plantarflexion and a decrease in dorsiflexion, resulting in a shift to larger MTP angles with mass (Fig. 3f; Suppl. Table 3).

Joint moments

Despite the small changes in joint rotation in the proximal hindlimb, we detected a decrease in magnitude of the dimensionless hip extensor and knee flexor moments with mass (Suppl. Fig. 4a, Suppl. Table 4), and an increase in magnitude of both joint moments with speed during the braking period of stance (Suppl. Fig. 4b). Maximum hip extensor moment and knee flexor moment were significantly influenced by the interaction between body mass and speed, suggesting that larger kangaroos increased the magnitude of the moments at a faster rate with speed compared to smaller kangaroos.

Joint work and power

The MTP was the only joint which did predominantly negative work. The MTP did more negative work with speed, while net MTP work decreased with both mass and speed (Suppl. Fig. 5g,h; Suppl. Fig. 6g,h; Suppl. Table 6). The MTP transition from negative work to positive work at ~80% stance, as the back of the foot started to leave the ground. Conversely, the knee did almost no negative work, and the hip did very little (Fig. 5; Suppl. Fig. 5; Suppl. Fig. 6). Net work slightly increased with mass and speed in the hip, while at the knee, net work increased only with speed (Suppl. Table 6).

Supplementary Videos

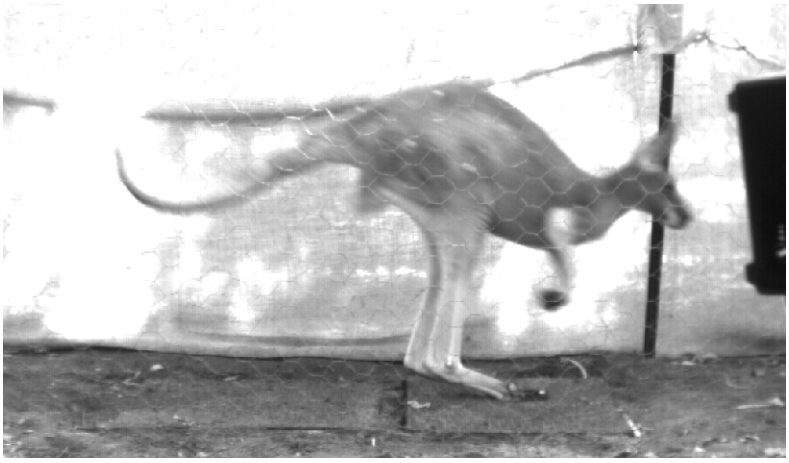

Suppl Video 1: A red kangaroo hopping on the force plate during data collection.

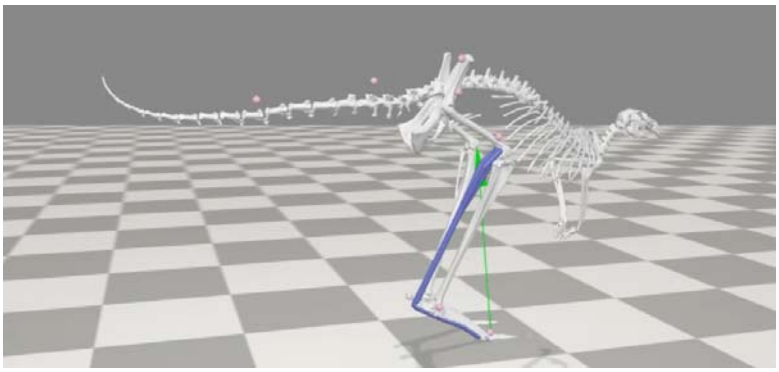

Suppl Video 2: Driving the musculoskeletal model with a recorded hopping trial. The gastrocnemius and plantaris muscle-tendon unit (Achilles) is shown in blue. The GRF appears in green. Markers associating the recorded kangaroos with the model are in pink.

Supplementary Figures

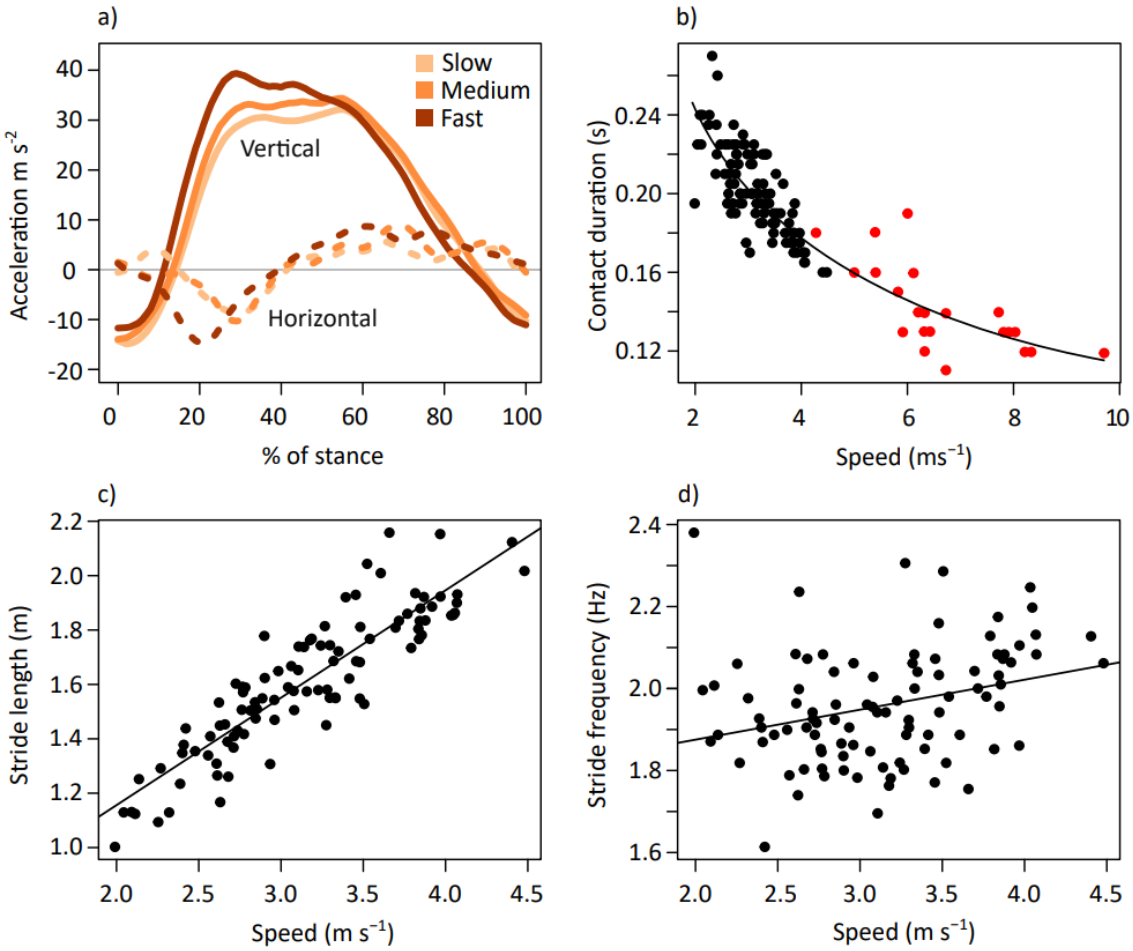

Suppl Figure 1: a) Mean vertical and horizontal components of whole body acceleration for kangaroos in the slow, medium and fast subsets (respectively: 2.52±0.25 m s^{-1}, 3.11±0.16 m s^{-1}, 3.79±0.27 m s^{-1}). (b) Ground contact duration across hopping speeds from current study (black circles) and for red kangaroos reported in Kram and Dawson (1998) (red circles). Regression equation: $t_c = 0.342 \text{speed}^{-0.477}$ where t_c is contact duration and s is hopping speed. (c) Relationship between stride length and speed, and (d) stride frequency and speed.

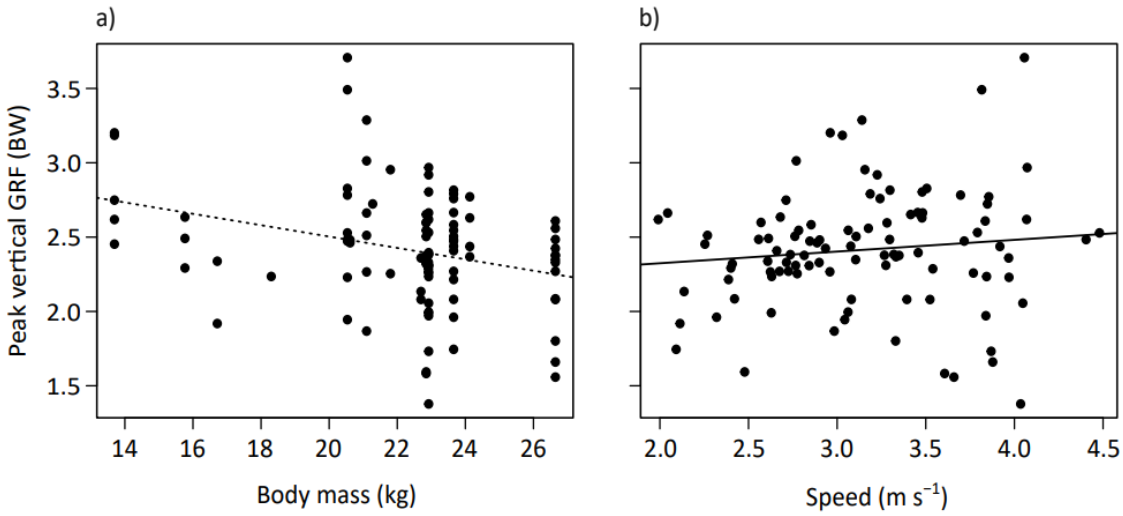

Suppl Figure 2: (a) Relationship between peak vertical GRF as a multiple of body weight (BW) with body mass and (b) with speed. Dotted line is insignificant and solid line is significant, see Table 2 for interaction.

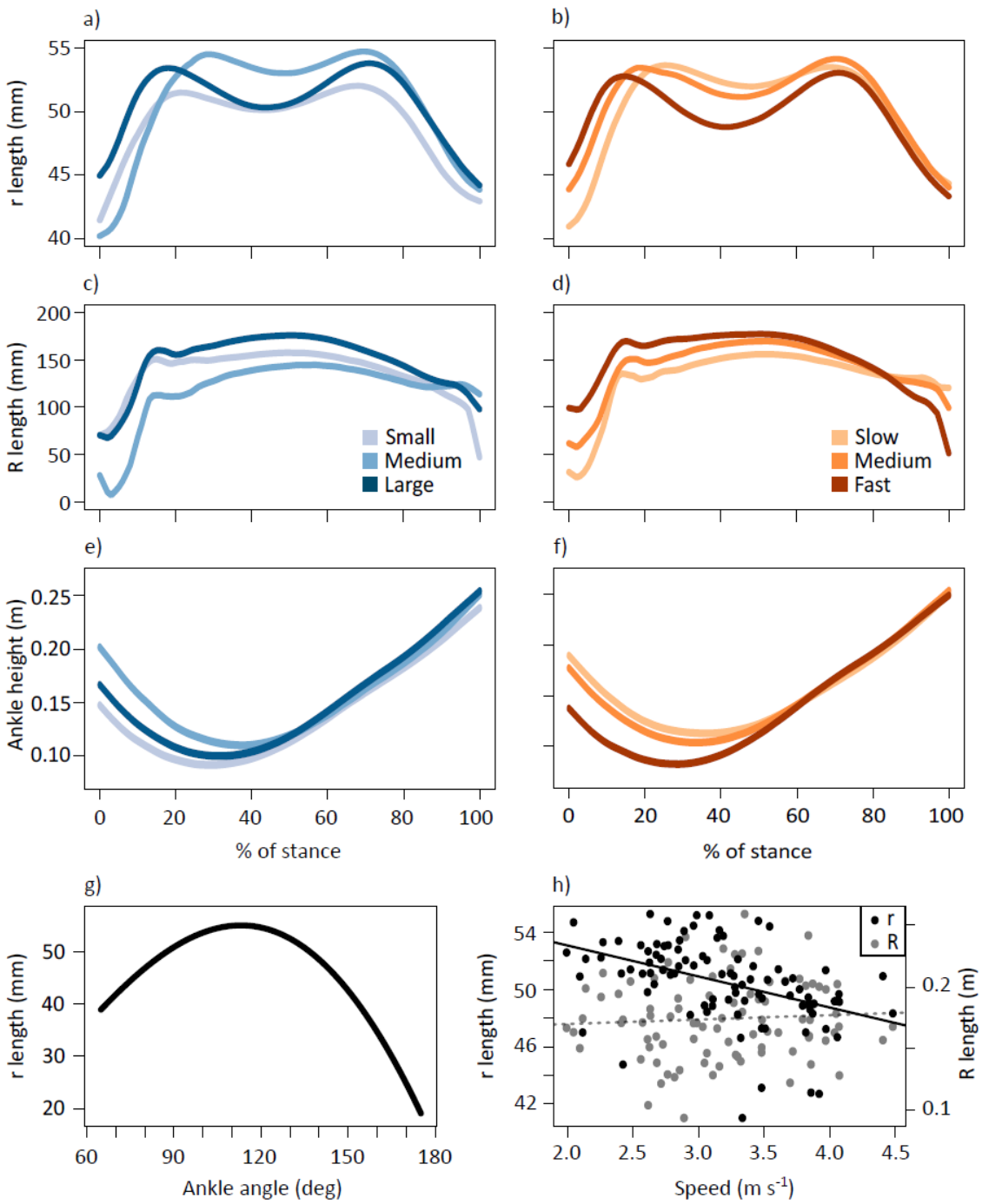

Suppl Figure 3: Average time-varying gastrocnemius and plantaris muscle moment arm, *r*, grouped by (a) body mass and (b) speed; external moment arm to the ankle, *R*, grouped by (c) body mass and (d) speed. Vertical displacement of the ankle marker from the ground throughout stance grouped by (e) body mass and (f) speed. Ankle angles and corresponding *r* arm length (g). Length of the *r* and *R* moment arms at midstance at different speeds (h). Body mass subsets: small 17.6±2.96 kg, medium 21.5±0.74 kg, large 24.0±1.46 kg. Speed subsets: slow 2.52±0.25 m s^{-1}, medium 3.11±0.16 m s^{-1}, fast 3.79±0.27 m s^{-1}.

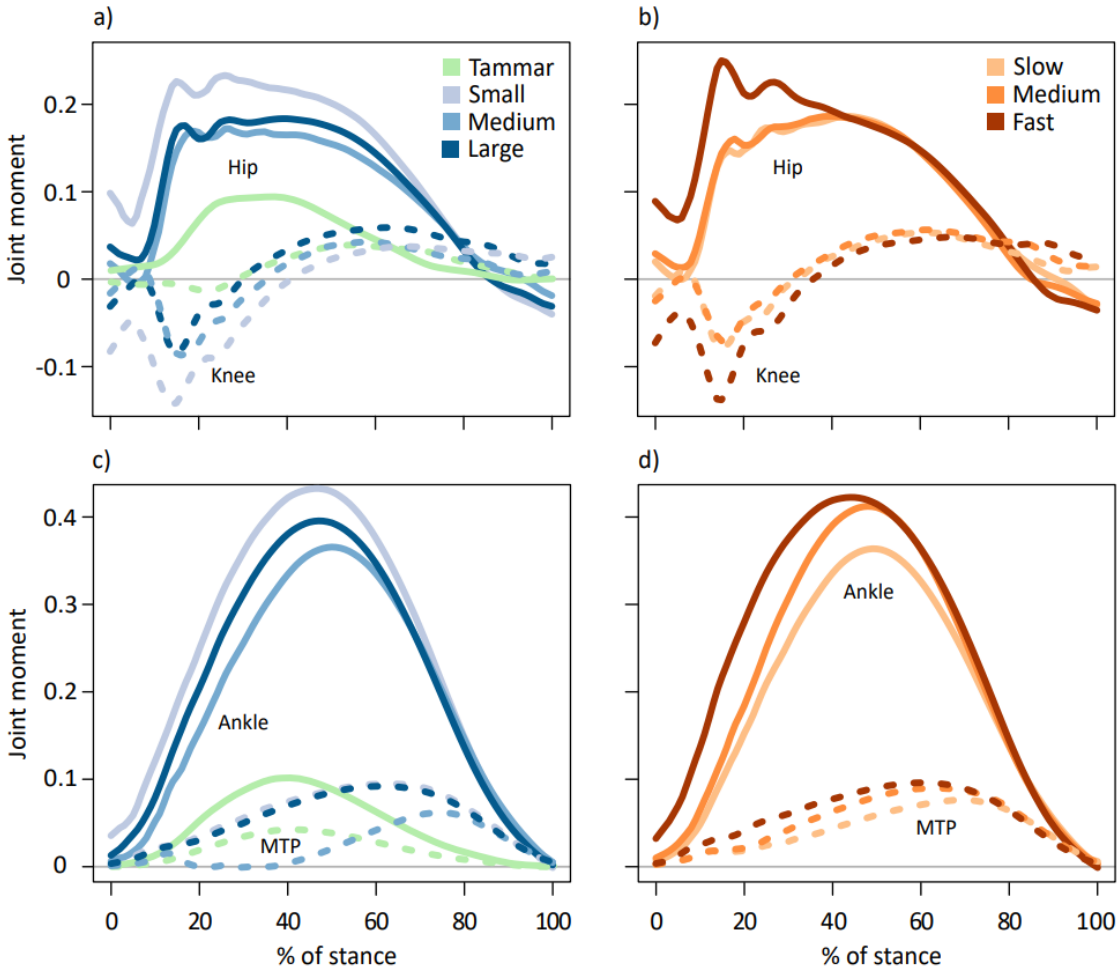

818

819 **Suppl Figure 4**: Average time-varying net joint moments (dimensionless, as moments were divided
820 by body weight * leg length) for the hip (solid lines) and knee (dotted lines) displayed for kangaroos
821 grouped by (a) body mass and (b) speed. Average time-varying net joint moments (dimensionless)
822 for the ankle (solid lines) and metatarsophalangeal (MTP; dotted lines) joints displayed for
823 kangaroos grouped by (c) body mass and (d) speed. Data for tammar wallabies was also included
824 (McGowan *et al.* 2005) in green. Peak ankle moment occurred at 47.37±4.91 % of the stance phase.
825 Positive values represent extensor moments and negative values represent flexor moments. Body
826 mass subsets: small 17.6±2.96 kg, medium 21.5±0.74 kg, large 24.0±1.46 kg. Speed subsets: slow
827 2.52±0.25 m s^{-1}, medium 3.11±0.16 m s^{-1}, fast 3.79±0.27 m s^{-1}.

828

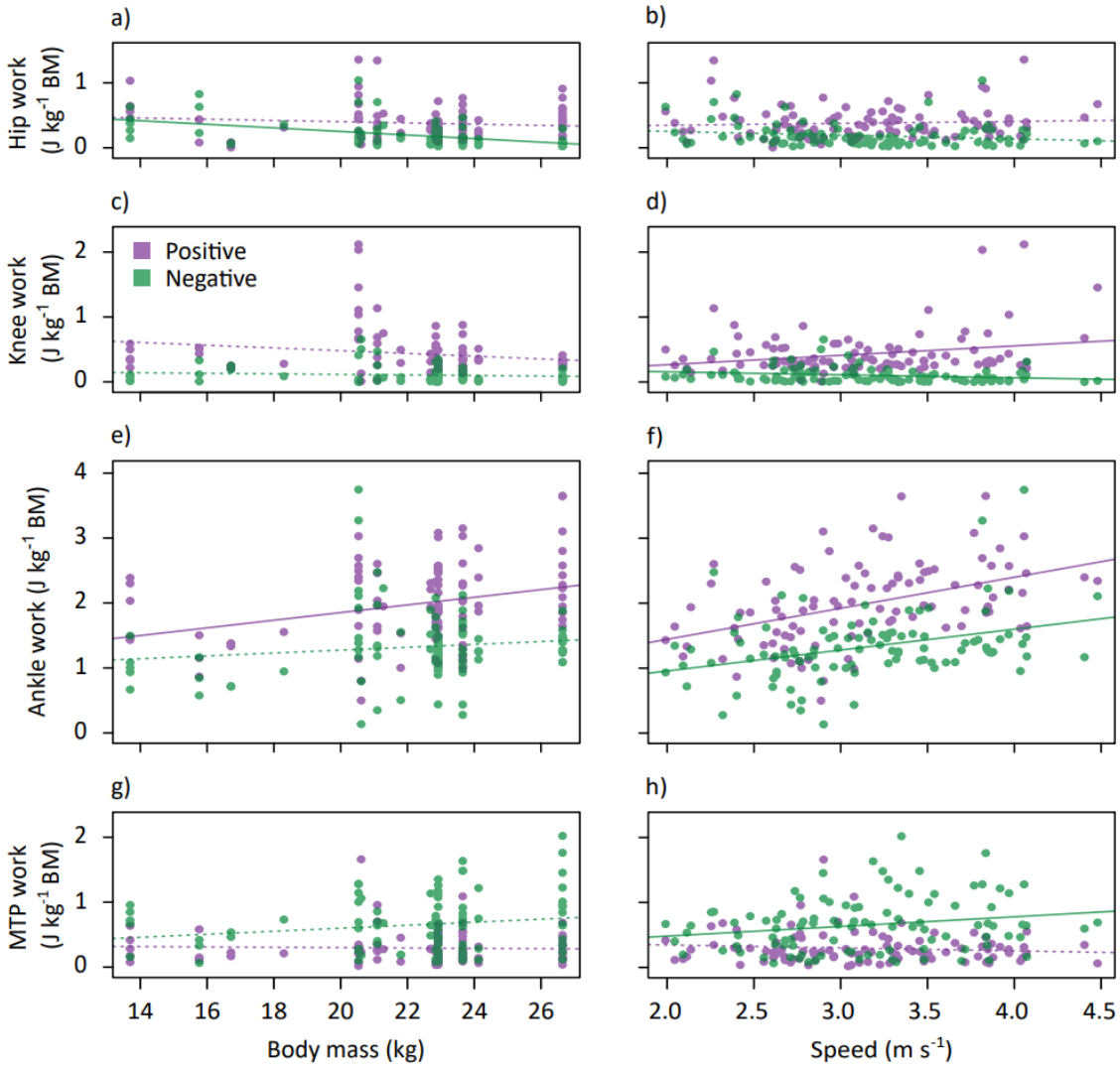

Suppl Figure 5: Positive (purple) and negative (green) joint work over stance for the hip, knee, ankle and MTP plotted against body mass (a,c,e,g) and speed (b,d,f,h). Solid lines represent significant trends, dotted lines are not significant (see Suppl Table 6).

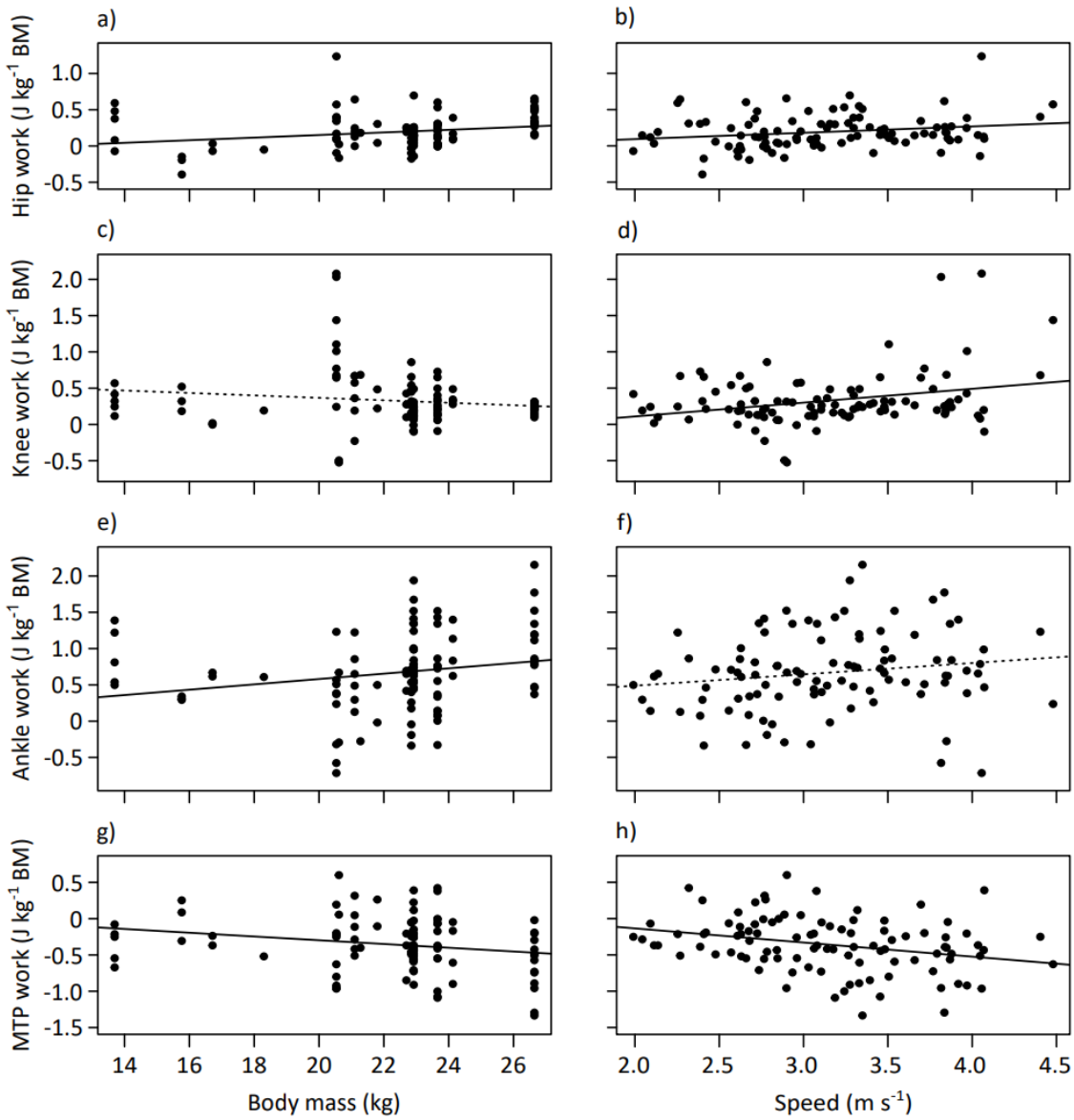

Suppl Figure 6: Net joint work for the hip, knee, ankle and MTP joint over stance plotted against body mass (a,c,e,g) and speed (b,d,f,h). Solid lines represent significant trends, dotted lines are not significant (see Suppl Table 6).

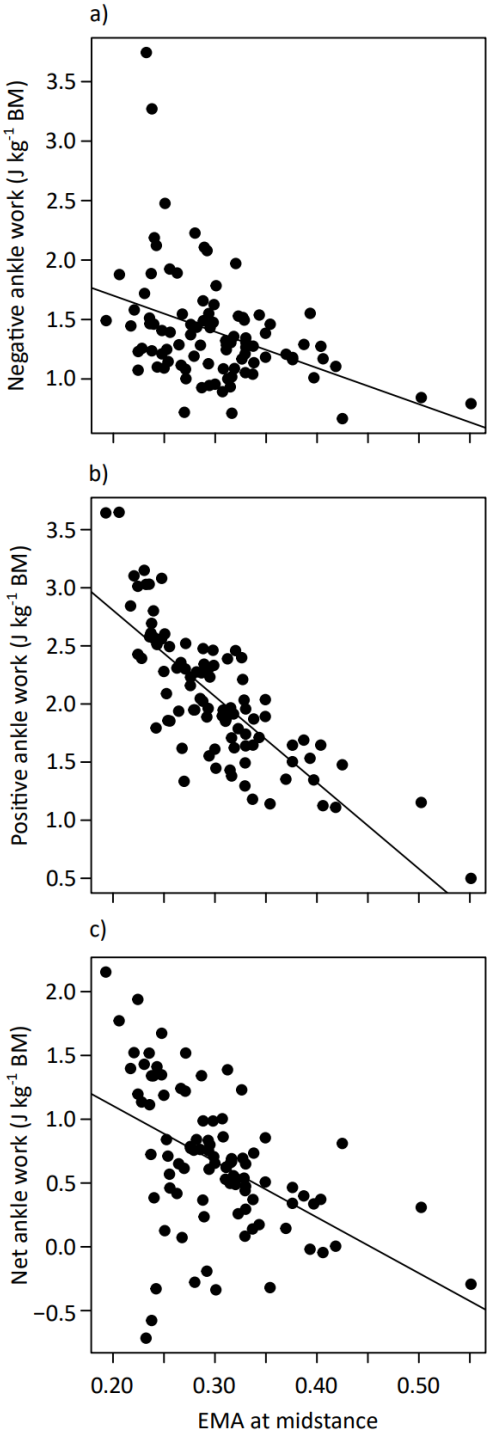

Suppl Figure 7: Negative (a) (B=-3.04, SE=0.75, P<0.001, R^2=0.155), positive (b) (B=-7.42, SE=0.61, P<0.001, R^2=0.622), and net ankle work (c) (B=-4.37, SE=0.84, P<0.001, R^2=0.230) plotted against EMA at 50% of stance.

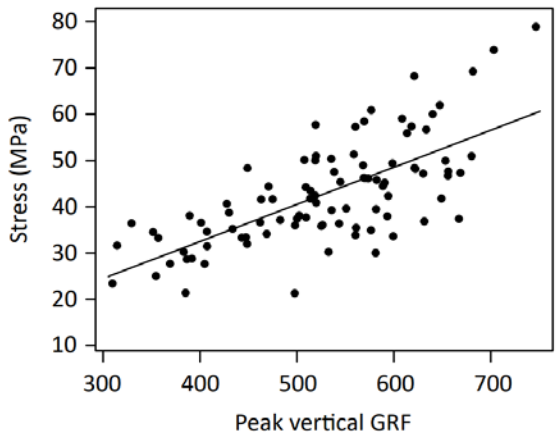

Suppl Figure 8: Peak vertical ground reaction force (GRF) plotted against tendon stress (B=0.080, SE=0.009, P<0.001, R^2=0.486).

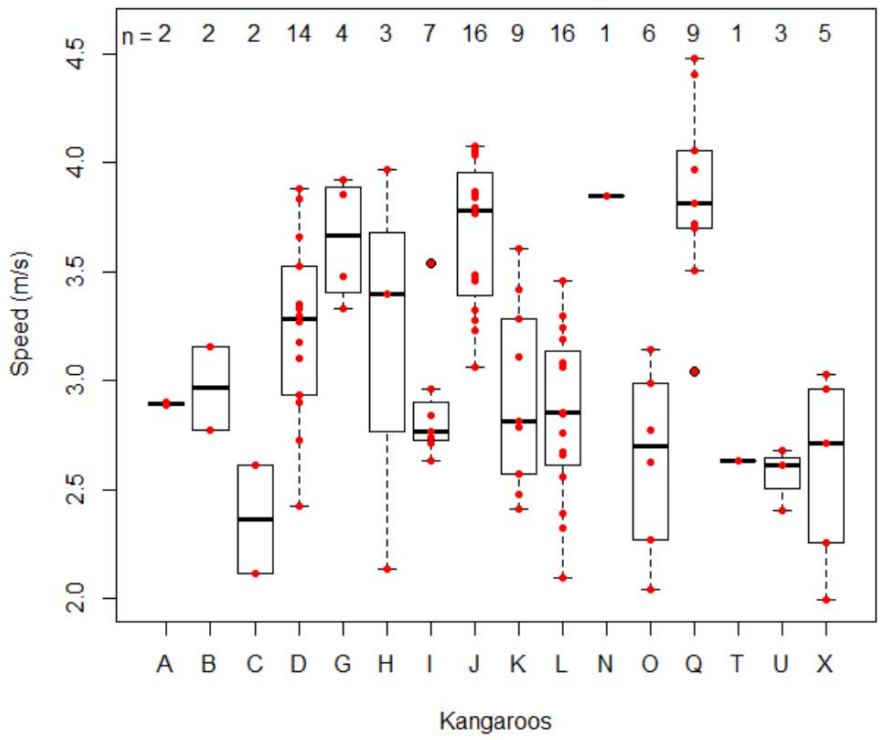

Suppl Figure 9: Distribution of trial speeds and number of trials (n) per kangaroo (6.25±5.02 trials per kangaroo).

Supplementary Tables

Suppl Table 1: Stride parameter multiple linear regression results as slopes, standard errors and P-values. Models with a significant interaction are displayed in full, and as a simplified model without the interaction term included (marked *). The fit of the model is represented by R^2 and relationships are considered significant at P<0.05.

	Interaction			Body mass			Speed			R^2
	β	SE	P	β	SE	P	β	SE	P	
Maximum vertical acceleration (m s^{-2})	-1.19	0.567	0.038	2.72	1.64	0.100	32.5	12.5	0.011	0.190
Maximum vertical acceleration (m s^{-2})*				-0.673	0.294	0.024	6.32	1.60	0.000	0.152
Minimum vertical acceleration (m s^{-2})				0.221	0.208	0.290	-0.268	1.13	0.814	0.012
Maximum horizontal acceleration (m s^{-2})				-0.036	0.296	0.903	0.159	1.61	0.922	0.000
Minimum horizontal acceleration (m s^{-2})				0.407	0.370	0.275	-6.05	2.02	0.003	0.087
Contact duration (ms)				2.87	0.393	0.000	-34.2	2.12	0.000	0.735
Stride length (m)				0.014	0.004	0.001	0.376	0.020	0.000	0.815
Stride frequency (Hz)	0.022	0.008	0.007	-0.082	0.023	0.001	-0.392	0.180	0.032	0.303
Stride frequency (Hz)*				-0.019	0.004	0.000	0.102	0.023	0.000	0.245

Suppl Table 2: Ground reaction force and centre of pressure (CoP) multiple linear regression results as slopes, standard errors and P-values. Models with a significant interaction are displayed in full, and as a simplified model without the interaction term included (marked *). The fit of the model is

	Interaction			Body mass			Speed			R^2
	β	SE	P	β	SE	P	β	SE	P	
Normalised peak GRF (BW)	-0.055	0.024	0.026	0.111	0.070	0.117	1.34	0.535	0.014	0.172
Normalised peak GRF (BW)*				-0.045	0.013	0.001	0.142	0.068	0.040	0.128
Peak vertical GRF (N)	-11.5	5.31	0.032	47.9	15.4	0.002	281	117	0.019	0.332
Peak vertical GRF (N)*				15.0	2.76	0.000	28.4	14.9	0.060	0.299
Peak braking GRF (N)	4.87	2.04	0.019	-14.8	5.90	0.014	-130	45.0	0.005	0.218
Peak braking GRF (N)*				-0.917	1.07	0.392	-23.2	5.76	0.000	0.172
Peak propulsive GRF (N)				2.03	0.818	0.015	21.5	4.42	0.000	0.285
CoP location at midstance (mm)				-0.123	1.54	0.937	-15.2	8.34	0.071	0.036
CoP location at midstance corrected for phalanx size (mm)				-0.437	17.0	0.980	-62.7	91.9	0.497	0.005

represented by R^2 and relationships are considered significant at $P<0.05$.

Suppl Table 3: Crouch factor (CF) and kinematics multiple linear regression results as slopes, standard errors and P-values. Models with a significant interaction are displayed in full, and as a simplified model without the interaction term included (marked *). The fit of the model is represented by R^2 and relationships are considered significant at $P<0.05$.

	Interaction			Body mass			Speed			R^2
	β	SE	P	β	SE	P	β	SE	P	
Maximum CF				-2.19	1.07	0.043	-15.8	5.74	0.007	0.122
Minimum CF				-2.45	0.885	0.007	-1.53	4.76	0.749	0.064
Change in CF				0.256	0.661	0.699	-14.2	3.55	0.000	0.129
Pelvis pitch ROM (deg)	0.935	0.298	0.002	-2.60	0.862	0.003	-19.9	6.58	0.003	0.100
Pelvis pitch ROM (deg)*				0.066	0.159	0.677	0.534	0.858	0.535	0.008
Hip ROM (deg)				-0.488	0.212	0.024	0.490	1.15	0.670	0.052
Minimum hip flexion (deg)				-0.655	0.315	0.040	0.703	1.70	0.681	0.043
Maximum hip flexion (deg)				-0.167	0.260	0.520	0.213	1.40	0.880	0.004
Knee ROM (deg)	-1.31	0.520	0.013	2.88	1.50	0.058	28.6	11.5	0.014	0.154
Knee ROM (deg)*				-0.850	0.272	0.002	-0.120	1.47	0.935	0.098
Minimum knee flexion (deg)	-1.72	0.649	0.010	3.76	1.88	0.048	39.5	14.3	0.007	0.162
Minimum knee flexion (deg)*				-1.13	0.34	0.001	1.95	1.84	0.294	0.101
Maximum knee flexion (deg)				-0.277	0.265	0.299	2.07	1.43	0.152	0.026
Ankle ROM (deg)				1.02	0.166	0.000	1.63	0.899	0.073	0.339
Peak ankle plantarflexion (deg)				-0.173	0.240	0.474	-3.87	1.30	0.004	0.104
Peak ankle dorsiflexion (deg)				-1.19	0.198	0.000	-5.49	1.07	0.000	0.466
MTP ROM (deg)				-0.098	0.259	0.707	7.16	1.40	0.000	0.219
Peak MTP plantarflexion (deg)				0.875	0.306	0.005	5.64	1.65	0.001	0.216
Peak MTP dorsiflexion (deg)				0.973	0.221	0.000	-1.52	1.20	0.205	0.166

874

875 **Suppl Table 4**: Multiple linear regression results of dimensionless peak joint moments as slopes,
876 standard errors and P-values. Models with a significant interaction are displayed in full, and as a
877 simplified model without the interaction term included (marked *). The fit of the model is
878 represented by R^2 and relationships are considered significant at $P<0.05$.

	Interaction			Body mass			Speed			R^2
	β	SE	P	β	SE	P	β	SE	P	
Hip extensor moment	-0.020	0.006	0.001	0.049	0.018	0.007	0.525	0.136	0.000	0.268
Hip extensor moment*				-0.009	0.003	0.010	0.079	0.018	0.000	0.184
Knee extensor moment				0.000	0.001	0.766	0.003	0.008	0.721	0.003
Knee flexor moment	0.020	0.005	0.000	-0.048	0.015	0.002	-0.487	0.116	0.000	0.264
Knee flexor moment*				0.008	0.003	0.007	-0.060	0.015	0.000	0.158
Ankle extensor moment				-0.004	0.004	0.256	0.043	0.020	0.036	0.048
MTP extensor moment				-0.001	0.002	0.767	0.000	0.013	0.986	0.001

879

880

Suppl Table 5: Tendon stress and EMA multiple linear regression results as slopes, standard errors and P-values. Models with a significant interaction are displayed in full, and as a simplified model without the interaction term included (marked *). The fit of the model is represented by R^2 and

	Interaction			Body mass			Speed			R^2
	β	SE	P	β	SE	P	β	SE	P	
r at midstance (mm)				-0.063	0.088	0.477	-1.88	0.474	0.000	0.173
R at midstance (mm)				3.49	1.03	0.001	-0.93	5.59	0.869	0.117
EMA at midstance				-6.64	1.98	0.001	-11.0	10.7	0.310	0.142
Peak tendon stress (MPa)				1.03	0.385	0.008	5.61	2.08	0.008	0.168
Normalised peak tendon stress				-0.048	0.018	0.008	0.258	0.096	0.008	0.107
Peak tendon stress timing %stance				-0.151	0.154	0.328	-3.13	0.831	0.000	0.159
Ankle height from ground (mm)				-0.298	0.706	0.674	-23.0	3.81	0.000	0.295

relationships are considered significant at $P<0.05$.

Suppl Table 6: Joint net positive, negative and net work simple linear regression (lm(joint work ~ mass), lm(joint work ~ speed)) results as slopes, standard errors and P-values. Work is normalised by body mass (BM). The fit of the model is represented by R^2 and relationships are considered significant at P<0.05.

	Body mass				Speed			
	β	SE	P	R^2	β	SE	P	R^2
Hip pos	-0.010	0.008	0.238	0.014	0.030	0.044	0.497	0.005
Hip neg	-0.027	0.005	0.000	0.225	-0.058	0.031	0.066	0.034
Hip net	0.018	0.007	0.018	0.055	0.087	0.041	0.034	0.045
Knee pos	-0.021	0.011	0.052	0.038	0.145	0.057	0.013	0.061
Knee neg	-0.004	0.004	0.267	0.013	-0.046	0.020	0.026	0.050
Knee net	-0.017	0.012	0.169	0.019	0.191	0.064	0.003	0.084
Ankle pos	0.059	0.019	0.003	0.087	0.478	0.097	0.000	0.197
Ankle neg	0.022	0.017	0.200	0.017	0.321	0.087	0.000	0.122
Ankle net	0.037	0.017	0.037	0.044	0.156	0.095	0.102	0.027
MTP pos	-0.003	0.008	0.743	0.001	-0.046	0.043	0.286	0.012
MTP neg	0.023	0.014	0.089	0.029	0.149	0.073	0.044	0.041
MTP net	-0.026	0.012	0.035	0.045	-0.194	0.064	0.003	0.086

Suppl Table 7: Positive, negative and net joint work multiple linear regression results as slopes, standard errors and P-values. Work is normalised by body mass (BM). Models with a significant interaction are displayed in full, and as a simplified model without the interaction term included (marked *). The fit of the model is represented by R^2 and relationships are considered significant at $P<0.05$.

Joint work (J kg^{-1} BM)	Interaction			Body mass			Speed			R^2
	β	SE	P	β	SE	P	β	SE	P	
Hip positive				0.046	0.045	0.307	-0.012	0.008	0.161	0.025
Hip negative				-0.021	0.029	0.472	-0.026	0.005	0.000	0.229
Hip net				0.067	0.042	0.110	0.015	0.008	0.058	0.080
Knee positive	-0.072	0.020	0.000	1.766	0.431	0.000	0.175	0.057	0.003	0.241
Knee positive*				0.187	0.057	0.002	-0.030	0.011	0.006	0.133
Knee negative				-0.043	0.021	0.045	-0.002	0.004	0.570	0.053
Knee net	-0.073	0.022	0.002	1.818	0.491	0.000	0.179	0.064	0.007	0.219
Knee net*				0.230	0.064	0.001	-0.028	0.012	0.021	0.133
Ankle positive				0.424	0.099	0.000	0.039	0.018	0.038	0.232
Ankle negative	-0.080	0.032	0.015	2.052	0.707	0.005	0.234	0.093	0.013	0.176
Ankle negative*				0.311	0.091	0.001	0.007	0.017	0.671	0.123
Ankle net	0.122	0.033	0.000	-2.551	0.732	0.001	-0.315	0.096	0.001	0.173
Ankle net*				0.112	0.097	0.250	0.031	0.018	0.084	0.057
MTP positive				-0.045	0.044	0.312	0.000	0.008	0.956	0.012
MTP negative				0.125	0.075	0.101	0.017	0.014	0.217	0.056
MTP net				-0.170	0.066	0.011	-0.018	0.012	0.149	0.106

Suppl Table 8: The mean and standard deviation of joint work for all trials. Positive, negative and net work is presented for each joint.

Joint work (J kg^{-1} BM)	Mean	SD
Hip positive	0.38	0.246
Hip negative	0.187	0.178
Hip net	0.193	0.235
Knee positive	0.432	0.334
Knee negative	0.104	0.117
Knee net	0.328	0.375
Ankle positive	1.99	0.613
Ankle negative	1.324	0.525
Ankle net	0.666	0.542
MTP positive	0.294	0.242
MTP negative	0.652	0.42
MTP net	-0.358	0.377

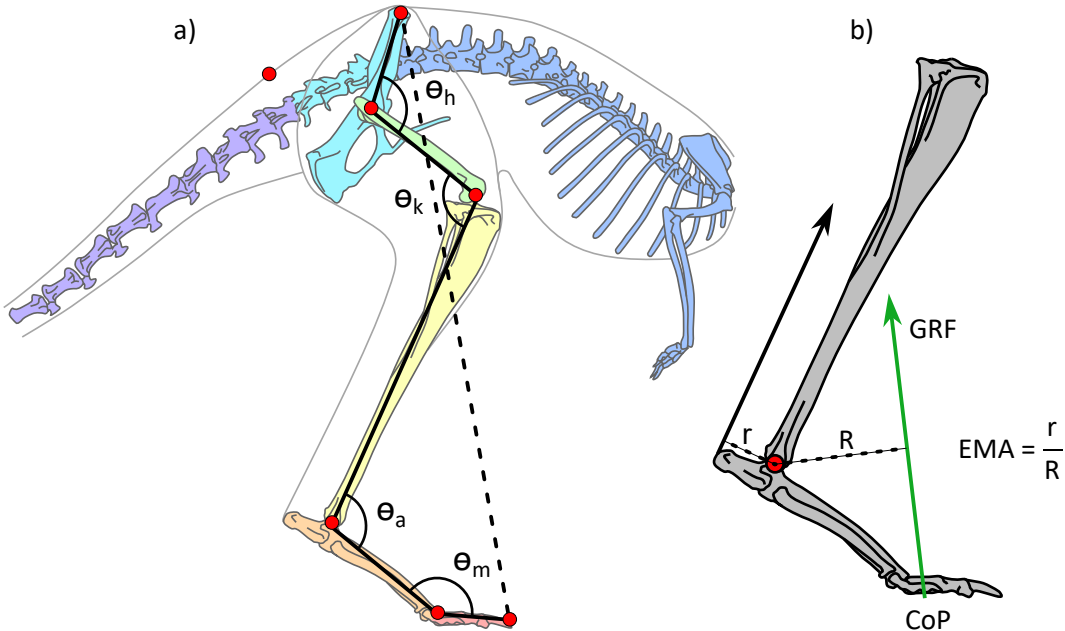
a)
θh
θk
θa
θm
b)
GRF
r
R
EMA = r/R
CoP

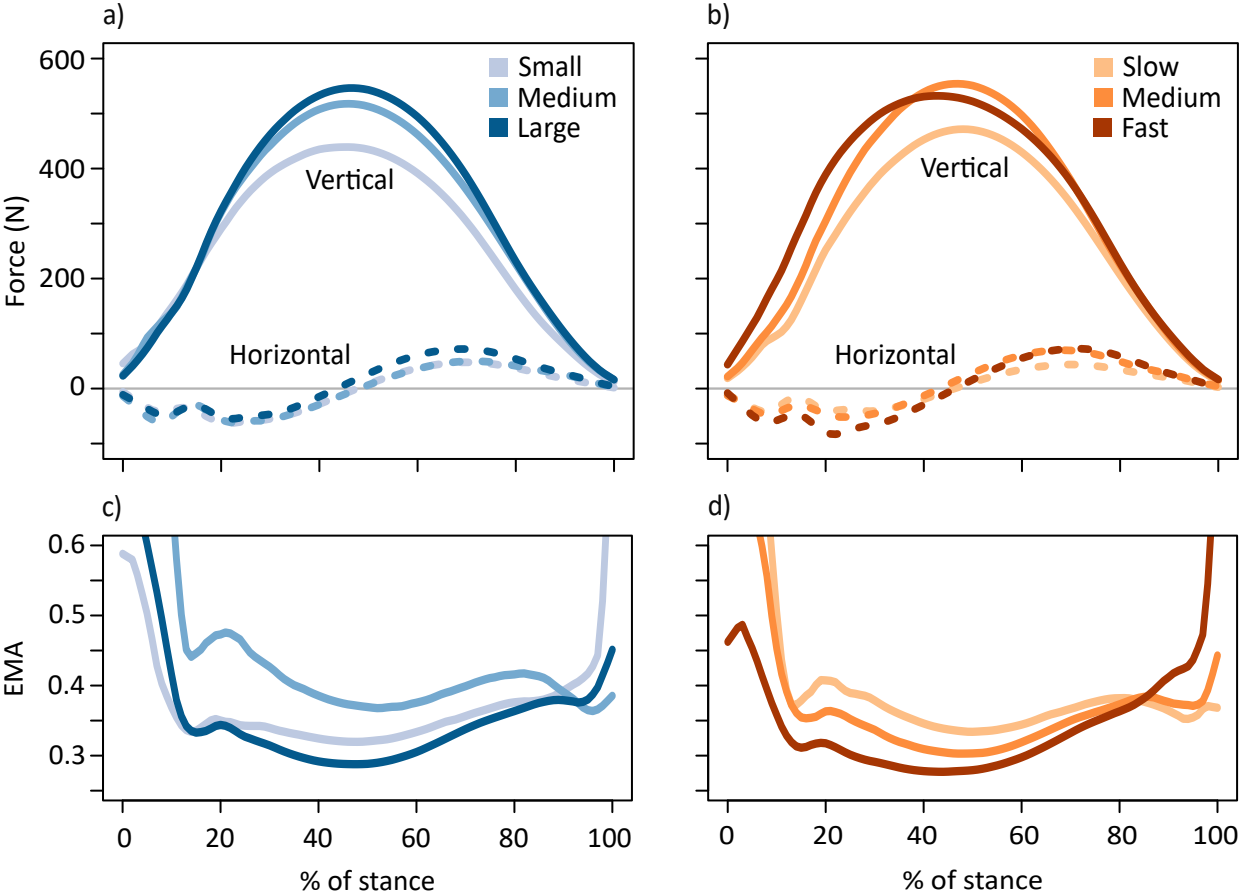
a)
b)
c)
d)
Small
Medium
Large
Slow
Medium
Fast
Vertical
Horizontal
Force (N)
600
400
200
0
EMA
0.6
0.5
0.4
0.3
0
20
40
60
80
100
% of stance

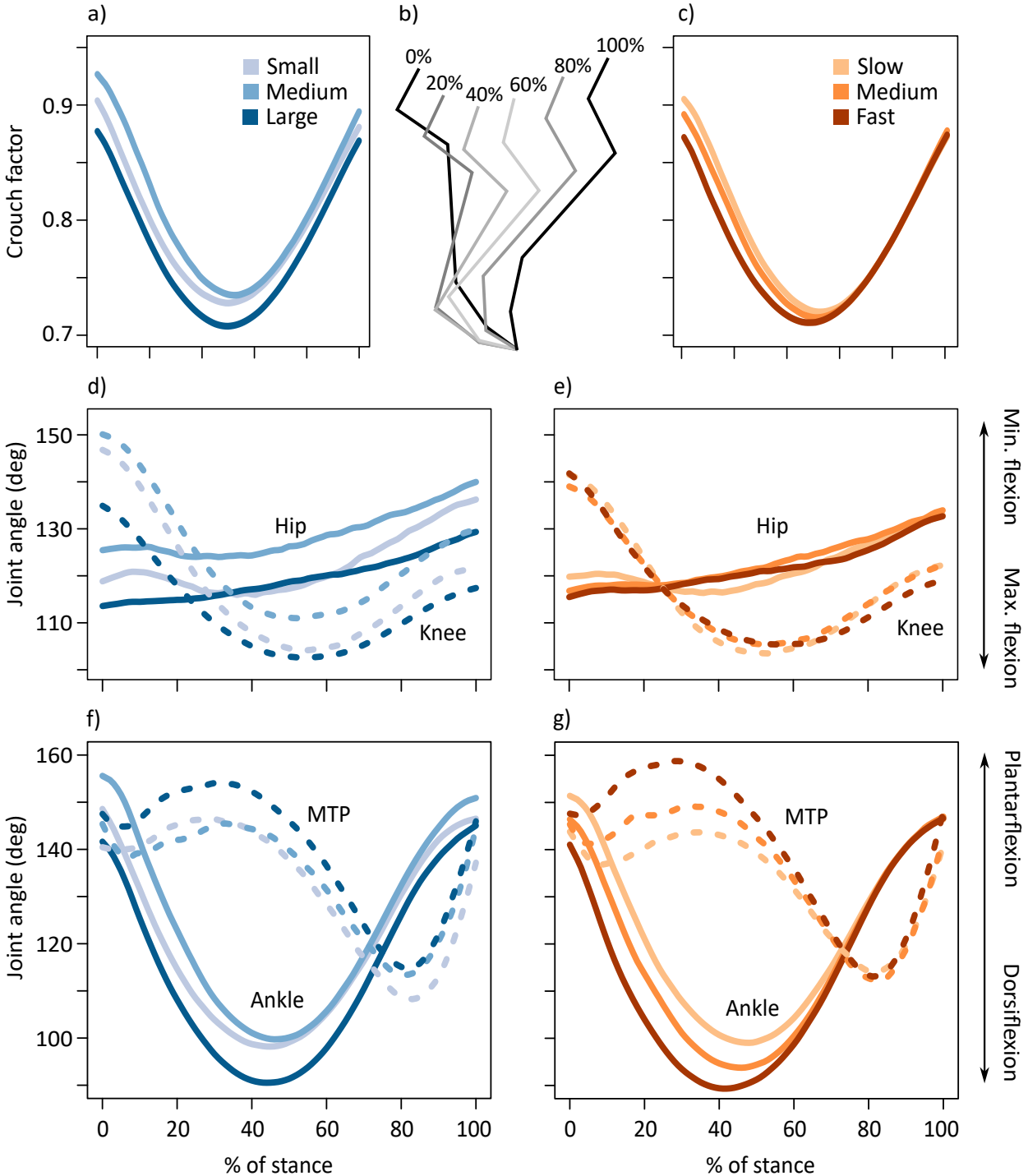
a)
b)
c)
Small
Medium
Large
Crouch factor
0.9
0.8
0.7
0%
20%
40%
60%
80%
100%
Slow
Medium
Fast
d)
e)
Joint angle (deg)
150
130
110
Hip
Knee
Min. flexion
Max. flexion
f)
g)
160
140
120
100
MTP
Ankle
Plantarflexion
Dorsiflexion
0
20
40
60
80
100
% of stance

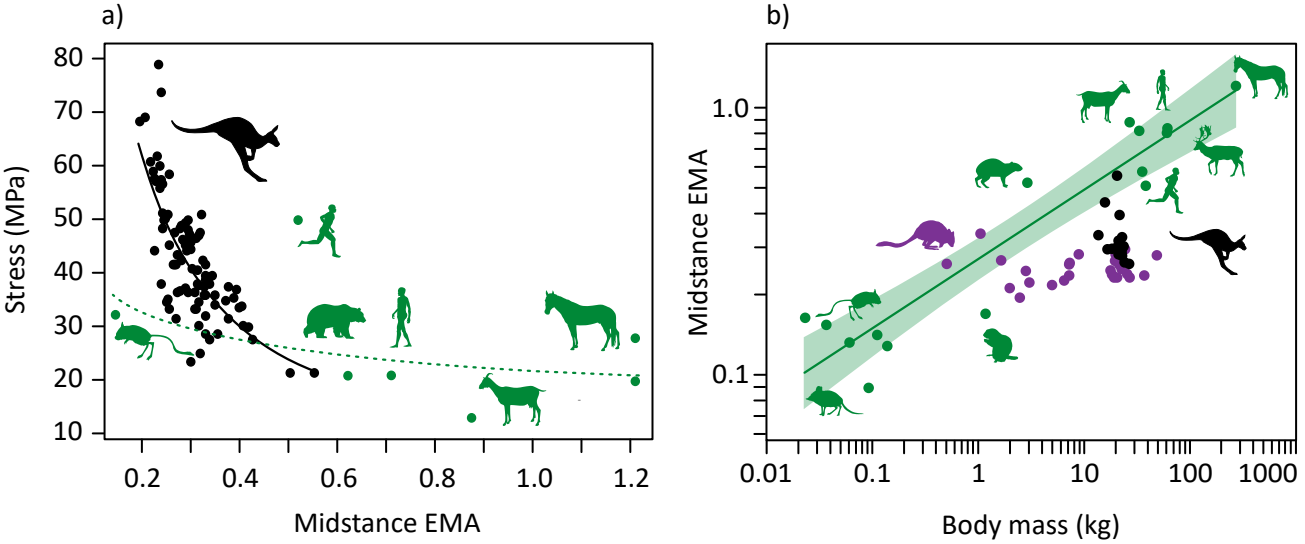
a)
Stress (MPa)
80
70
60
50
40
30
20
10
0.2
0.4
0.6
0.8
1.0
1.2
Midstance EMA
b)
Midstance EMA
1.0
0.1
0.01
0.1
1
10
100
1000
Body mass (kg)

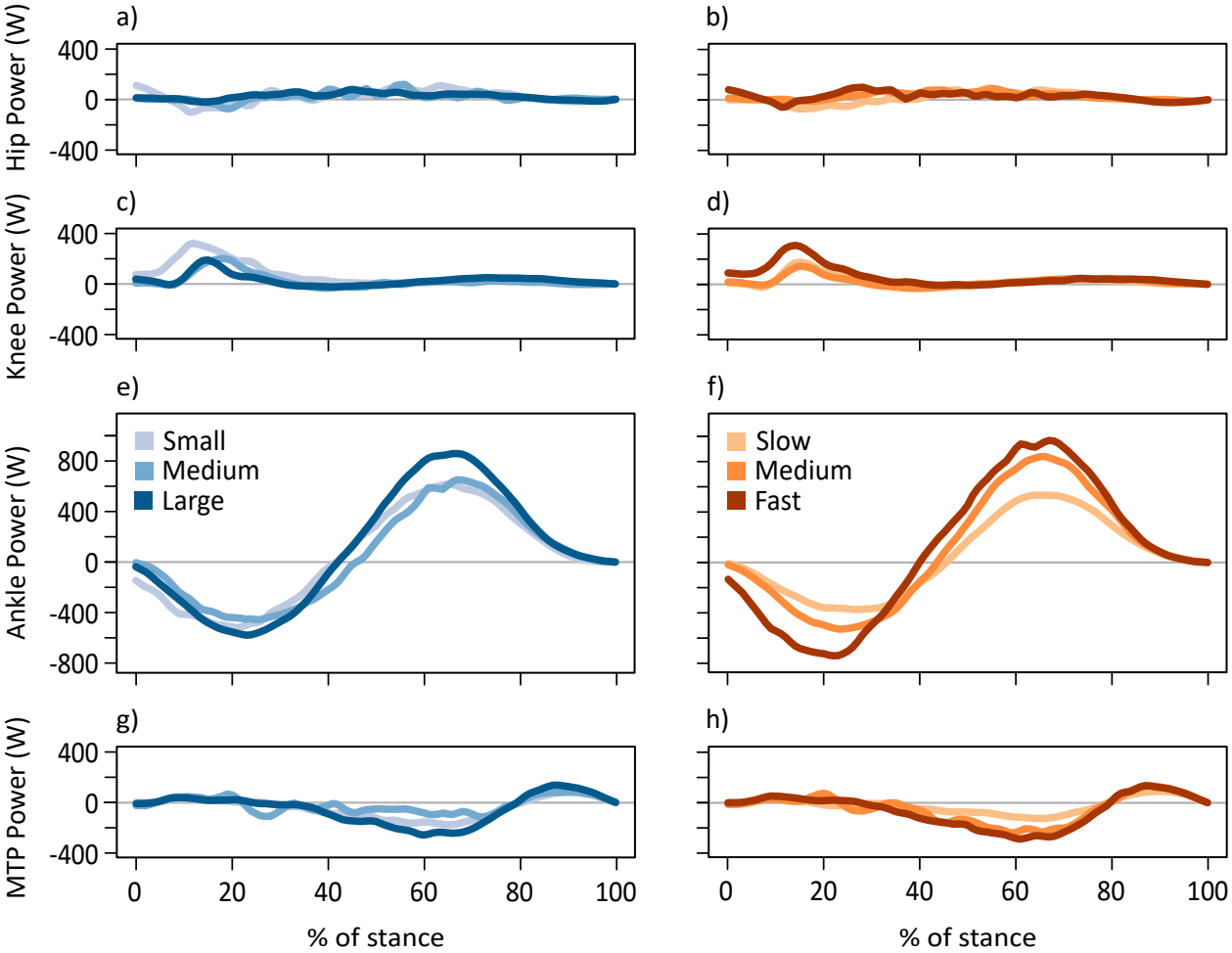
a)
b)
c)
d)
e)
f)
g)
h)
Hip Power (W)
Knee Power (W)
Ankle Power (W)
MTP Power (W)
400
0
-400
800
-800
Small
Medium
Large
Slow
Medium
Fast
0
20
40
60
80
100
% of stance
% of stance

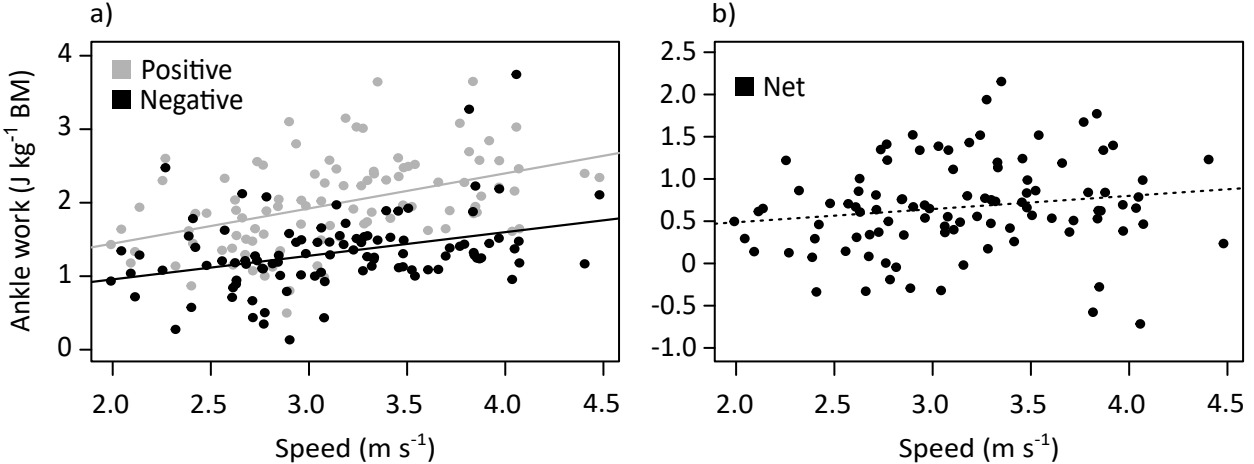
a)
Positive
Negative
Ankle work (J kg-1 BM)
4
3
2
1
0
2.0
2.5
3.0
3.5
4.0
4.5
Speed (m s-1)
b)
Net
2.5
2.0
1.5
1.0
0.5
0
-0.5
-1.0
2.0
2.5
3.0
3.5
4.0
4.5
Speed (m s-1)

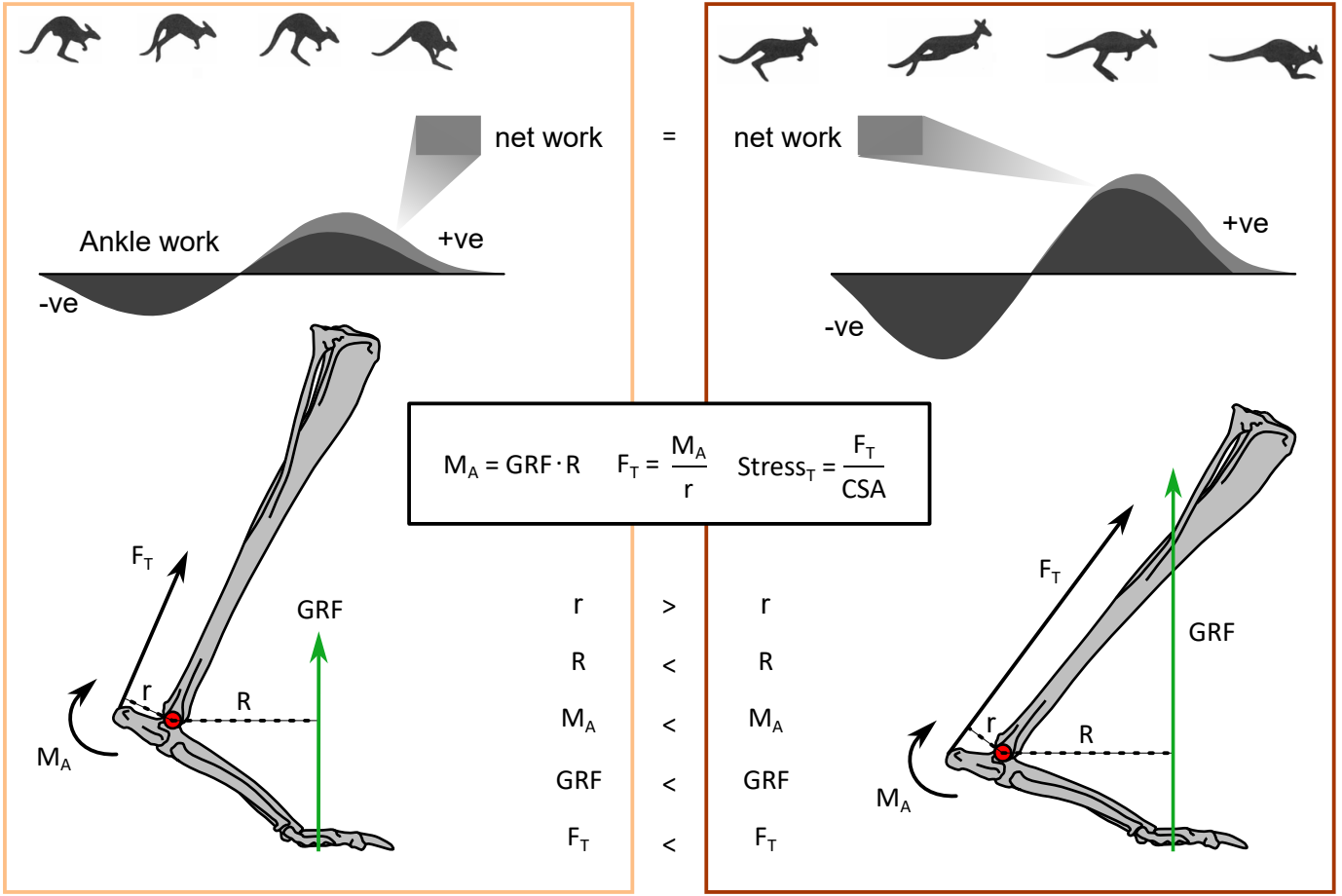
net work
=
net work
Ankle work
+ve
-ve
+ve
-ve
$M_A = GRF \cdot R$
$F_T = \frac{M_A}{r}$
$Stress_T = \frac{F_T}{CSA}$
F_T
GRF
r
R
M_A
r > r
R < R
M_A < M_A
GRF < GRF
F_T < F_T
F_T
GRF
r
R
M_A